OPEN ACCESS Freely available online PLoS one

Identification of Hepatic Niche Harboring Human Acute Lymphoblastic Leukemic Cells via the SDF-1/CXCR4 Axis

Itaru Kato[1,2], Akira Niwa[1,2], Toshio Heike[2], Hisanori Fujino[2], Megumu K. Saito[1,2], Katsutsugu Umeda[3], Hidefumi Hiramatsu[2], Mamoru Ito[4], Makiko Morita[5], Yoko Nishinaka[5], Souichi Adachi[5], Fumihiko Ishikawa[6], Tatsutoshi Nakahata[1,2]*

1 Department of Clinical Application, Center for iPS Cell Research and Application, Kyoto University, Kyoto, Japan, **2** Department of Pediatrics, Graduate School of Medicine, Kyoto University, Kyoto, Japan, **3** Centre for Stem Cell Research, Brown Foundation Institute of Molecular Medicine for the Prevention of Human Diseases, The University of Texas Health Science Center at Houston, Houston, Texas, United States of America, **4** Central Institute for Experimental Animals, Kanagawa, Japan, **5** Human Health Sciences, Graduate School of Medicine, Kyoto University, Kyoto, Japan, **6** Research Unit for Human Disease Models, RIKEN Research Center for Allergy and Immunology, Kanagawa, Japan

Abstract

In acute lymphoblastic leukemia (ALL) patients, the bone marrow niche is widely known to be an important element of treatment response and relapse. Furthermore, a characteristic liver pathology observed in ALL patients implies that the hepatic microenvironment provides an extramedullary niche for leukemic cells. However, it remains unclear whether the liver actually provides a specific niche. The mechanism underlying this pathology is also poorly understood. Here, to answer these questions, we reconstituted the histopathology of leukemic liver by using patients-derived primary ALL cells into NOD/SCID/Yc ^{null} mice. The liver pathology in this model was similar to that observed in the patients. By using this model, we clearly demonstrated that bile duct epithelial cells form a hepatic niche that supports infiltration and proliferation of ALL cells in the liver. Furthermore, we showed that functions of the niche are maintained by the SDF-1/CXCR4 axis, proposing a novel therapeutic approach targeting the extramedullary niche by inhibition of the SDF-1/CXCR4 axis. In conclusion, we demonstrated that the liver dissemination of leukemia is not due to nonselective infiltration, but rather systematic invasion and proliferation of leukemic cells in hepatic niche. Although the contribution of SDF-1/CXCR4 axis is reported in some cancer cells or leukemic niches such as bone marrow, we demonstrated that this axis works even in the extramedullary niche of leukemic cells. Our findings form the basis for therapeutic approaches that target the extramedullary niche by inhibiting the SDF-1/CXCR4 axis.

Citation: Kato I, Niwa A, Heike T, Fujino H, Saito MK, et al. (2011) Identification of Hepatic Niche Harboring Human Acute Lymphoblastic Leukemic Cells via the SDF-1/CXCR4 Axis. PLoS ONE 6(11): e27042. doi:10.1371/journal.pone.0027042

Editor: Felipe Prosper, Clinica Universidad de Navarra, Spain

Received November 26, 2010; **Accepted** October 9, 2011; **Published** November 1, 2011

Funding: This work was supported by a Grant-in-Aid for Scientific Research (S) (19109006) from the Ministry of Education, Science, Technology, Sports and Culture of Japan, and Health and Labour Science Research Grants from the Ministry of Health, Labour and Welfare of Japan. The funders had no role in study design, data collection and analysis, decision to publish, or preparation of the manuscript.

Competing Interests: The authors have declared that no competing interests exist.

* E-mail: tnakaha@kuhp.kyoto-u.ac.jp

Introduction

Acute lymphoblastic leukemia (ALL) is the most common malignant disease in children[1]. Although accumulated improvements in treatment regimens have raised the 5-year survival rate to as high as 80% in pediatric patients[2], a poor prognosis is still expected for a minority of patients with various risk factors and those with ALL relapses. In particular, relapsed ALL has an overall survival rate of only 30%[3].

Recent studies about leukemic cells and niche correlation highlight the importance of therapeutically targeting the bone marrow (BM) microenvironment [4,5]. The BM niche provides survival and growth factors for leukemic cells, modulates their responses to chemotherapies and may even contribute to the relapse of the disease. But little is known about the extramedullary niche of leukemia.

Organ involvement varies with the type of neoplastic cell[6]. Such cells find their own appropriate microenviromental conditions in particular tissues for survival and proliferation[6]. The widespread involvement of extramedullary organs is characteristic of leukemia. Although leukemic cells can easily disseminate to all organs by traveling in the peripheral blood, the most striking changes are restricted in organs such as the liver and spleen. Even after leukemic cells seem to disappear after treatment, residual leukemic cells are thought to be released from BM and extramedullary niche, eventually causing recurrence of the disease [7]. Consequently, investigation of the interactions between leukemic cells and the niche at extramedullary sites is a crucial component in the management and overcome of leukemia; however, little is known about the role of extramedullary niche in harboring leukemic cells. Specifically, whether extramedullary sites actually provide a specific niche, and the factors responsible for harboring leukemic cells in extramedullary niche remain unclear.

We previously developed a novel immunodeficient NOD/SCID/Yc ^{null} (NOG) mouse that provides significantly better human hematopoietic cell engraftment in the BM and extramedullary organs than other immunodeficient mice[8,9,10,11], and is capable of supporting the growth of human neoplastic cells[12]. In the present study, we introduced a human leukemic mouse

xenograft model using the NOG mice attended by extramedullary involvement without pre-conditioning (hereby referred to as the h-leukemic NOG model). Previous animal xeno-transplantation models for recapitulating human leukemia required preconditioning to avoid graft rejection [13,14]. However, these models are not appropriate for detailed pathological assessment of extramedullary microenvironments because preconditioning causes modification of the microenvironment such as upregulation of SDF-1 [15]. As the h-leukemic NOG model can reproduce leukemic extramedullary involvement without preconditioning, our approach provides a more sophisticated and physiological model suitable to study the interactions between leukemic cells and the host niche.

Leukemic cells preferentially infiltrate the liver, and the hepatomegaly is detected in as high as 30–50% of acute lymphoblastic leukemia (ALL) patients at diagnosis[16]. As hepatopathology of ALL is well characterized[17], but little is known about the molecular mechanisms that contribute to this pathology, we have focused on the liver for studying the role of extramedullary niche in sustaining leukemia.

In this paper, we have demonstrated that hepatomegaly and pathology in ALL patients are not only due to random infiltration but rather the result of SDF-1/CXCR4 axis-dependent migration and expansion of leukemic cells in the hepatic niche. Moreover, we have succeeded in suppressing post-chemotherapeutic leukemic regrowth in the hepatic niche by inhibiting the SDF-1/CXCR4 axis, thus resulting in an improvement in the overall survival. Although the contribution of SDF-1/CXCR4 axis is reported in some cancer cells [18,19] or leukemic niches such as bone marrow [20], we demonstrated that this axis works even in the extramedullary niche of leukemic cells. These results provide a better understanding of the mechanisms of the extramedullary dissemination and aid in the development of ALL therapies that target the extramedullary niche.

Results

Human leukemic cells can be serially reconstituted in NOG mice without pre-conditioning

To establish a xenograft murine model of human ALL without damage to the recipient niche (h-leukemic NOG model), we first injected 1×10^6 leukemic cells derived from primary BM of nine ALL children into the tail veins of untreated NOG mice (Table 1). Flow cytometric analysis of the BM revealed that eight of the nine leukemias engrafted in transplanted mice were detectable three weeks post-transplantation, and that BM chimerisms reached more than 40% of leukemic cells within 28 weeks in all engrafted cases (Figure 1A and Figure S1). Sequential H-E staining and immunohistochemical analysis of ALL #1 leukemic cell-engrafted humeri using anti-hCD45 antibodies demonstrated that hCD45-positive leukemic cells continued to reside within the BM (Figure 1B). Serial transplantation of leukemic cells from three representative cases into secondary and tertiary recipients demonstrated a conserved morphology (Figure 1C) and characteristic immunophenotypes (Figure 1D) in NOG mice. These results demonstrate the potential of our h-leukemic NOG model to recapitulate human ALL in NOG mice.

Liver pathology in the h-leukemic NOG model resembles that in leukemic patients

The h-leukemic NOG model showed the development of pale BM, hepatomegaly, and splenomegaly same as the original patient (Figure 2A and 2B), which was massively infiltrated with lymphoblasts (Figure S2). In the analysis of liver pathology, large clusters of leukemic cells were observed in the portal area of all cases analyzed (Figure 2C), consistent with the previously reported pathology of human ALL patients[17]. The same pathological results were obtained even after the intra-femoral injection of leukemic cells (Figure 2C).

Sequential analysis showed that small number of leukemic cells first localized around the bile ducts, and then developed into large clusters in the portal area. On the other hand, only single cells or small clusters were scattered throughout the sinusoidal areas (Figure 2D). These results suggest that our model recapitulates the histopathology of human ALL leukemic liver. Moreover, the data strongly indicate some specific mechanism by which portal areas attract and retain ALL leukemic cells.

Leukemic cells proliferated around liver bile duct epithelial cells

To confirm whether leukemic cells are proliferating after settling in the liver, we performed cell cycle analysis of leukemic cells harvested from the liver, PB, and BM. The liver and BM contained a substantial fraction of proliferating leukemic cells (Figure 3A and 3B), while leukemic cells in the PB were predominantly non-proliferating. *In vivo* immunohistochemical staining with BrdU also showed that human CD45- positive leukemic cells in the liver were in the proliferation phase (Figure 3C). Interestingly, significantly increased number of BrdU

Table 1. Patient and leukemia characteristics.

Patient ID	Age/Gender	Source	WBC (/μl)	BM blast (%)	Stage	Immunophenotype	Cytogenetics
ALL #1	7/M	BM	183600	81.5	Diagnosis	$CD45^+CD10^+CD19^+CD20^-$	Normal
ALL #2	1/F	BM	7700	10	Relapse	$CD45^+CD10^+CD19^+CD20^{partial}$	Normal
ALL #3	4/F	BM	10500	91	Diagnosis	$CD45^+CD10^+CD19^+CD20^-$	Hyperdiploid
ALL #4	7/M	BM	3700	84.7	Diagnosis	$CD45^+CD10^+CD19^+CD20^{partial}$	E2A/PBX
ALL #5	4/F	BM	800	43.2	Diagnosis	$CD45^+CD10^+CD19^+CD20^+$	TEL/AML-1
ALL #6	4/M	BM	323700	91	Diagnosis	$CD45^+CD10^+CD19^+CD20^-$	Hyperdiploid
ALL #7	9/F	BM	3800	92.5	Diagnosis	$CD45^+CD10^+CD19^+CD20^{partial}$	TEL/AML-1
ALL #8	2/M	BM	4300	75.4	Diagnosis	$CD45^+CD10^+CD19^+CD20^{partial}$	MLL/ENL
ALL #9	8/M	BM	29400	70	Diagnosis	$CD45^+CD10^+CD19^+CD20^{partial}$	Normal

M: male. F: female. BM: bone marrow. WBC: white blood cell.

doi:10.1371/journal.pone.0027042.t001

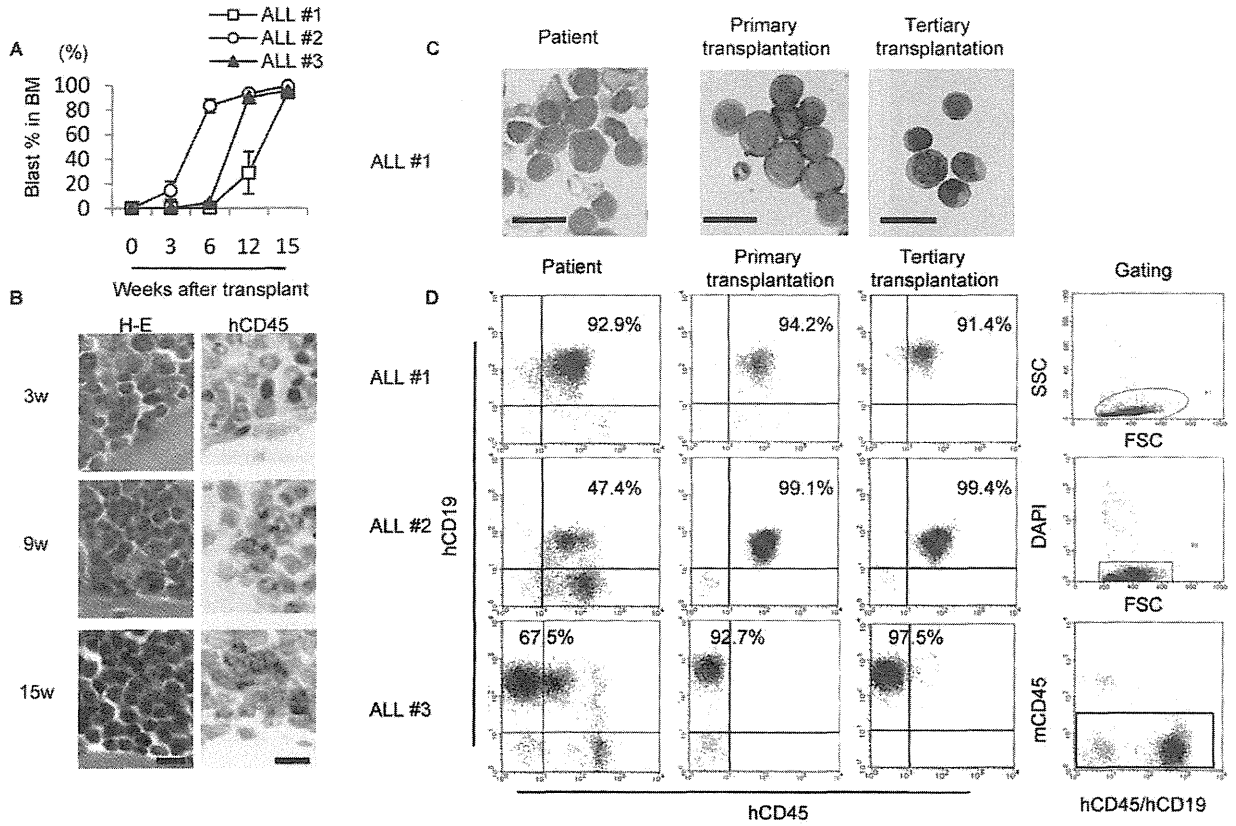

Figure 1. Leukemic cells can be engrafted to NOG mice without pre-conditioning. Morphology (May-Grunwald Giemsa staining) and immunophenotype of leukemic blasts remain stable during serial transplantation in NOG mice. (A) Sequential FACS analyses showing bone marrow engraftment after transplantation. Graphs show percentage of blast cells (hCD45 or hCD19 positive cells) in recipient BM ($n=3-6$ mice per case).Data are shown as means±S.D. (B) H-E staining and anti-hCD45 immunostaining showing increasing number of leukemic cells over time in the humerus of ALL#1 leukemic cell-recipient NOG mice. Scale bar, 10 μm. (C) Morphology and (D) immunophenotype of original patient blast cells (left row) and BM samples derived from murine primary and tertiary transplants of leukemic cells (middle and right rows). Debris (low forward scatter), dead cells (DAPI-positive), and mouse CD45 positive cells were excluded from analysis. Scale bar, 20 μm.
doi:10.1371/journal.pone.0027042.g001

positive leukemic cells were present in the portal areas compared to that in the sinusoidal areas (Figure 3D). Together, these results suggest that leukemic cells surrounding the bile ducts are not only anchored by bile duct epithelial cells, but also undergo proliferation around the bile duct epithelial cells.

The number of CXCR4 positive leukemic cells was significantly higher in the liver. Detailed description of liver pathology revealed the existence of a functional niche mediated by SDF-1/CXCR4 axis

Previous studies have demonstrated that several adhesion molecules and chemokines, including CXCR4, CD56, CD44, CCR7, and VLA-4, contribute to the harboring and proliferation of leukemic cells in the BM niche and may enhance niche-mediated resistance in leukemia [21,22,23,24,25]. To identify molecules involved in the pathology of the ALL leukemic liver, we analyzed their expression on leukemic cells harvested from the BM, liver, and spleen, in the three cases listed in Table 1. Flow cytometric analysis revealed that the percentage of CXCR4-positive leukemic cells was significantly higher in the liver than that in other organs (Figure 4A and 4B). Consistent with previous studies [15,26,27], SDF-1 was expressed on bile duct epithelial cells in the portal area of the h-leukemic NOG model (Figure 4C). Immunohistochemical analysis showed that CXCR4 positive leukemic cells were mainly distributed in the portal area, surrounding SDF-1 positive bile duct epithelial cells, but not in the sinusoidal area (Figure 4C). Moreover, proximity ligation assay confirmed the specific interaction between CXCR4 on leukemic cells and SDF1 (Figure S3). Therefore, these results strongly suggest that the SDF-1/CXCR4 axis plays a role in the hepatic niche of leukemic cells.

The SDF-1/CXCR4 axis stimulates not only migration, but also proliferation, of ALL leukemic cells *in vitro* and *in vivo*

The SDF-1/CXCR4 axis is a key factor in the migration and proliferation of various cells, including neoplastic cells *in vivo* [18,19,28]. Thus, we sought to directly examine the influence of the SDF-1/CXCR4 axis on leukemic cell migration and proliferation.

First, we performed a chemotaxis assay by stimulating CXCR4 with its ligand SDF-1 (Figure 5A). Leukemic cells harvested from the liver migrated avidly in response to SDF-1, and this migration

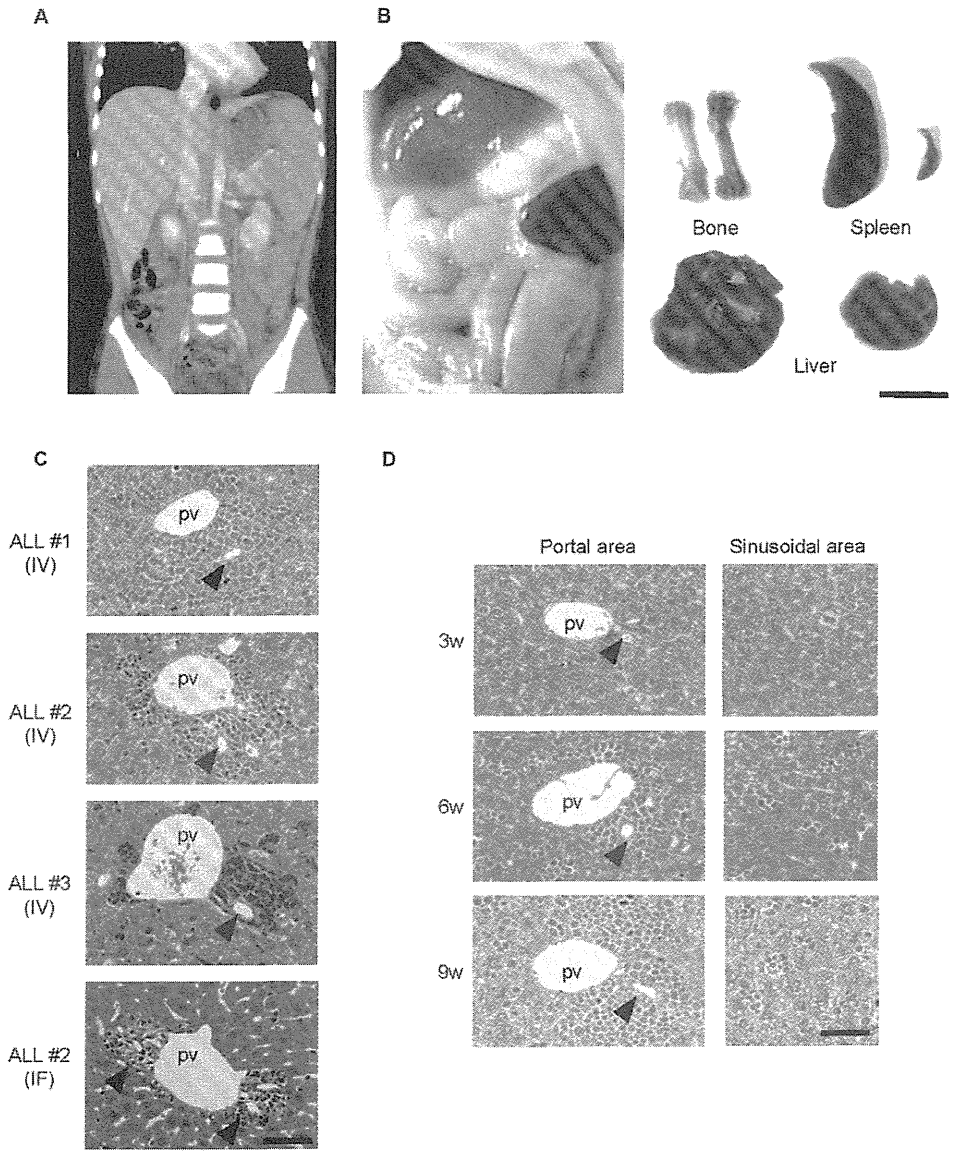

Figure 2. NOG recipient mice transplanted with ALL cells show a clinical leukemic pathology. (A) CT image of patient ALL#1 abdomen shows hepatosplenomegaly at diagnosis. (B) Macroscopic hepatosplenomegaly of the NOG recipient mouse transplanted with ALL#1 leukemic cells. Comparison of gross appearance of organs in normal mice (right-hand side) and leukemic NOG mice transplanted with ALL #1 leukemic cells (left-hand side). Pale femur and enlarged liver and spleen are shown. Scale bar, 1 cm. (C) In all ALL cases analyzed, the corresponding leukemic NOG recipients had large clusters of leukemic cells in portal area. Three representative cases of intra-vein injection and one case of intra-femoral injection are shown. Scale bar, 50 μm. (D) Sequential histopathological analysis of the liver of leukemic NOG mice transplanted with ALL#1 leukemic cells showed growth of leukemic cell clusters in portal areas (left column), but not sinusoidal areas (right column). Scale bar, 50 μm. pv; portal vein. IV; intra vein injection. IF; intra femoral injection. Arrowheads indicate bile ducts.
doi:10.1371/journal.pone.0027042.g002

was suppressed in the presence of AMD3100, a bicyclam molecule that antagonizes the binding of SDF-1 to CXCR4. Moreover, in a checkerboard assay, cell numbers increased along the positive SDF-1 gradient in a dose-dependent manner (Figure S4). These results confirm the effects of SDF-1 on the migration of leukemic cells.

We next performed a methylcellulose colony-forming assay to examine the effect of SDF-1/CXCR4 signaling on the proliferation of leukemic cells harvested from liver(Figure 5B). The addition of SDF-1 significantly increased the number of colonies, while treatment with AMD3100 counteracted the effect of SDF-1. Western blotting revealed that SDF-1 stimulation induced

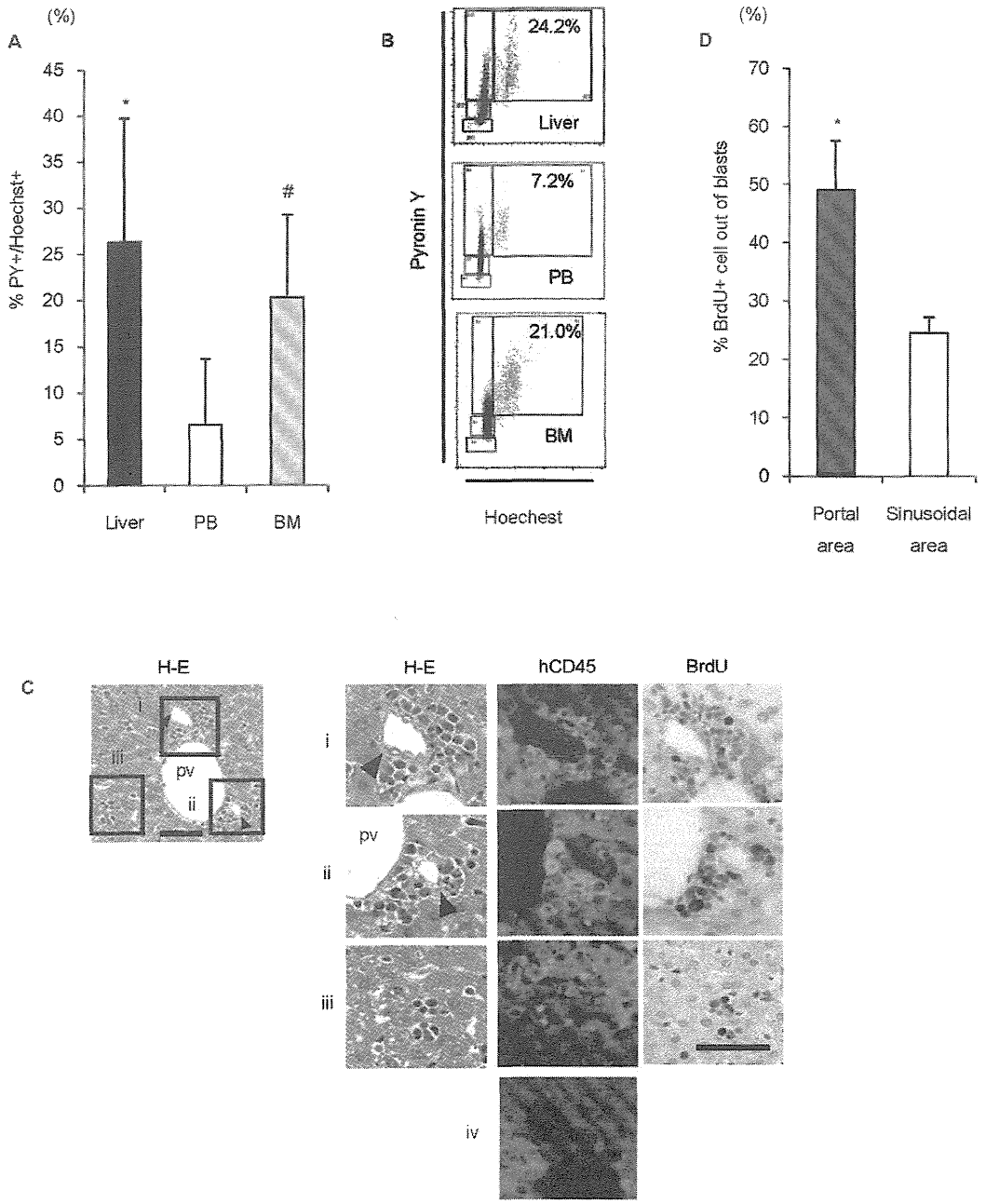

Figure 3. Human ALL cells preferentially proliferated around bile duct epithelial cells. (A) Frequency of S + G2/M phase leukemic cells in each organ of the mice (*$P = 0.019$, $^{\#}$ $P = 0.036$, Student's *t*-test, compared with leukemic cells in the peripheral blood, $n = 4-5$). Data are shown as mean±S.D. (B) Representative FACS panels of cell cycle analysis of leukemic cells in each tissue of the recipient mice. (C) H-E, hCD45, and BrdU staining of liver sections of h-leukemic NOG model. Bile duct epithelial cells were surrounded by large numbers of $hCD45^+$ leukemic cells in portal area (i and ii). A few $hCD45^+$ leukemic cells were observed as single cells or small clusters randomly distributed in the sinusoidal area (iii). Negative control (iv). Scale bar, 50 μm. pv; portal vein . Arrowheads indicate bile ducts. (D) Parcentage of BrdU-positive cells among blast cells in the portal and sinusoidal areas (*$P = 0.0015$, Student's *t*- test, $n = 4$). Data are shown as mean±S.D.
doi:10.1371/journal.pone.0027042.g003

phosphorylation of ERK1/2 and AKT which are known to be the important mediators of chemotaxis[26] and proliferation[20,29,30] of several cell types, and these phosphorylation were suppressed in the presence of AMD3100 (Figure 5C).

Next, we transplanted leukemic cells harvested from BM and liver, with different populations of CXCR4-positive cells, into NOG mice and compared the engraftment. Rapid growth of leukemic cells was observed in NOG mice transplanted with

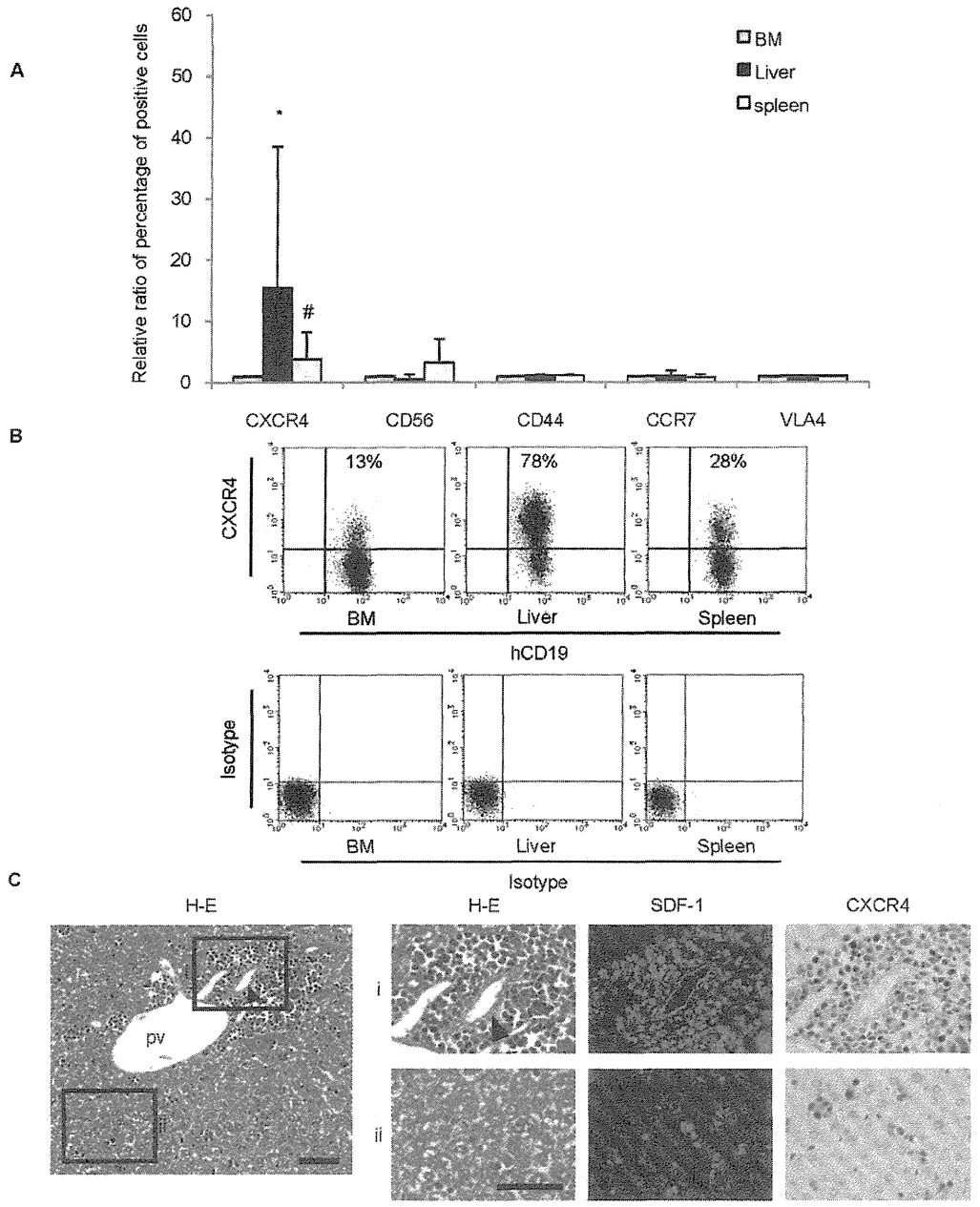

Figure 4. The ratio of CXCR4-positive leukemic cells was significantly higher in the liver. Bile duct epithelial cells were strongly positive for SDF-1 and surrounded by CXCR4 positive leukemic cells. (A) Relative ratio of percentage in positive cells of CXCR4, CD56, CD44, CCR7, and VLA4 out of leukemic cells harvested from liver and spleen compaired with leukemic cells from BM ($^{*}P = 0.0099$, $^{\#}P = 0.0091$, paired *t*-test. $n = 4-9$ mice per case. ALL#1, #2 and #3 were analyzed). Data are shown as mean±S.D. (B) Representative FACS panels of CXCR4 expression in leukemic cells from each organ. Leukemic cells in the liver show higher levels of CXCR4 expression than those in the BM. (C) Large number of leukemic cells were observed in the portal area, and bile duct epithelial cells are strongly positive for SDF-1. CXCR4-positive leukemic cells were present in large numbers around bile ducts. Portal area (i) and sinusoidal area (ii). Scale 50 μm. pv; portal vein. Arrowheads indicate bile ducts.
doi:10.1371/journal.pone.0027042.g004

leukemic cells harvested from the liver which contain large number of CXCR4-positive leukemic cells (Figure 5D).

Taken together, these data indicate that the SDF-1/CXCR4 axis stimulates not only migration but also proliferation of ALL leukemic cells *in vivo* and *in vitro*, and implied the importance of targeting the extramedullary microenvironment to prevent recurrence from emerging from minimal residual disease in the extramedullary microenvironment in ALL patients.

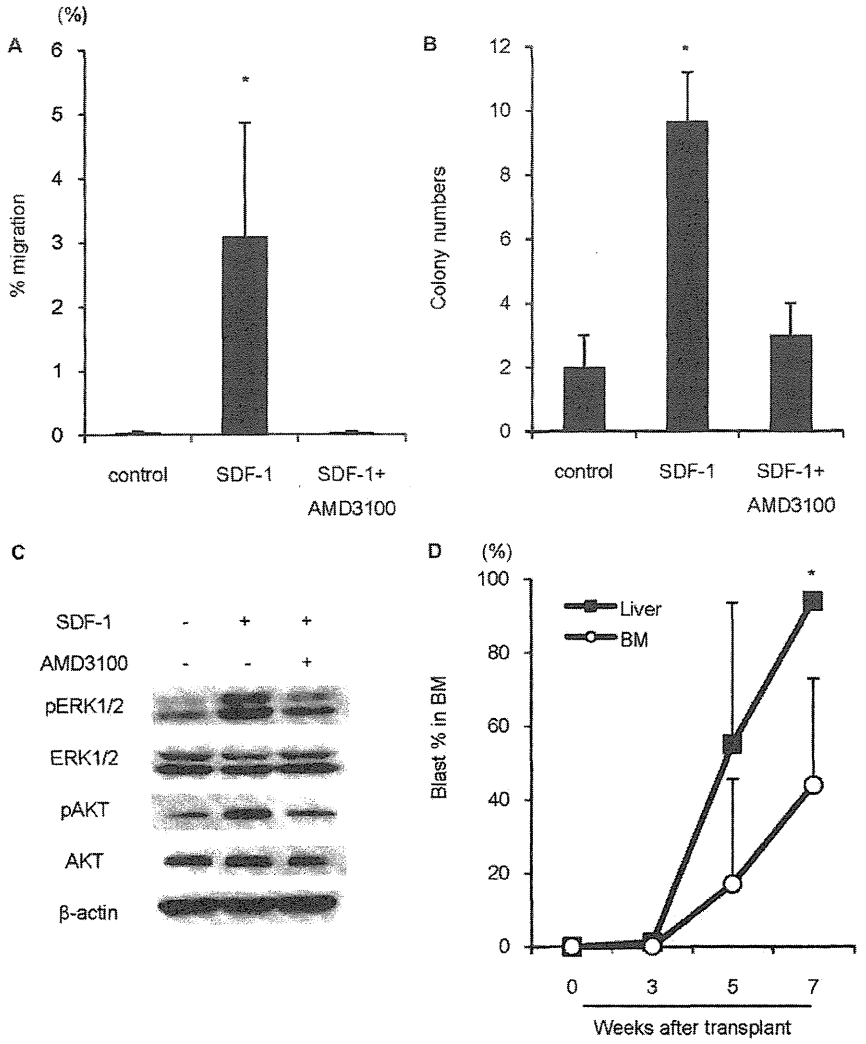

Figure 5. The signaling via SDF-1/CXCR4 axis stimulates migration and proliferation of leukemic cells. (A) Leukemic cells were plated onto upper chamber of transwell plates with 250 ng/ml SDF-1α in lower chamber, in presence or absence of AMD 3100 pretreatment. Results expressed as percentage of migrating cells to input cell number. (*$P = 0.014$, Student's *t*- test, $n = 4$). (B) Methylcellulose colony-forming assay to evaluate effect of SDF-1/CXCR4 signaling on leukemic cell proliferation. Addition of SDF-1α significantly increased leukemic colony numbers, and treatment with AMD3100 counteracted effect of SDF-1α (*$P = 0.0019$, Student's *t*-test, $n = 3$). (C) Phosphorylation of ERK1/2 (pERK1/2) and Akt (pAkt) was detected by Western blot analysis. β-actin was used as a loading control. (D) Sequential FACS analyses showing bone marrow engraftment after transplantation of leukemic cells harvested from BM and liver of ALL leukemic cell-transplanted mice. Graphs show percentage of blast cells in recipient BM (*$P = 0.0048$, Student's *t* -test, $n = 4-8$ mice per case). Data are shown as means±S.D.
doi:10.1371/journal.pone.0027042.g005

AMD3100 inhibited the *in vivo* dissemination of leukemic cells surrounding the bile ducts after chemotherapy and which thus led to the superior survival of the h-leukemic NOG mice

Finally, we examined the effects of inhibiting SDF-1/CXCR4 axis on leukemic cells in the hepatic niche. A single-dose of 75 mg/kg Ara-C in h-leukemic NOG mice significantly reduced leukemic cell numbers in PB (Figure 6A). Pathological analysis of the liver showed that leukemic cells accumulating around the portal area markedly decreased after 4 days of Ara-C treatment. However only a few remaining leukemic cells were observed mainly next to bile duct epithelial cells (Figure 6B). A cell cycle analysis of leukemic cells in the liver before and after Ara-C treatment revealed that the leukemic cells in the G2/M-phase of the cell cycle were preferentially eliminated, and that this was accompanied by the enrichment of the quiescent clones after chemotherapy (Figure S5). Within 3 weeks after treatment, the number of ALL cells returned to pre-treatment levels in the PB. We used this protocol as a model for chemotherapy-induced remission and recurrence.

To elucidate the effect of SDF-1/CXCR4 axis on leukemic cell clusters regrowth in the liver portal areas, we treated h-leukemic NOG mice with Ara-C and subsequently with AMD3100 or NS for seven days (Figure 6C). In control mice receiving NS, leukemic cell regrowth in the liver was observed primarily in the portal area by day 7 (Figure 6D, left panel). In contrast, in the treatment group receiving AMD3100, leukemic cell cluster regrowth was

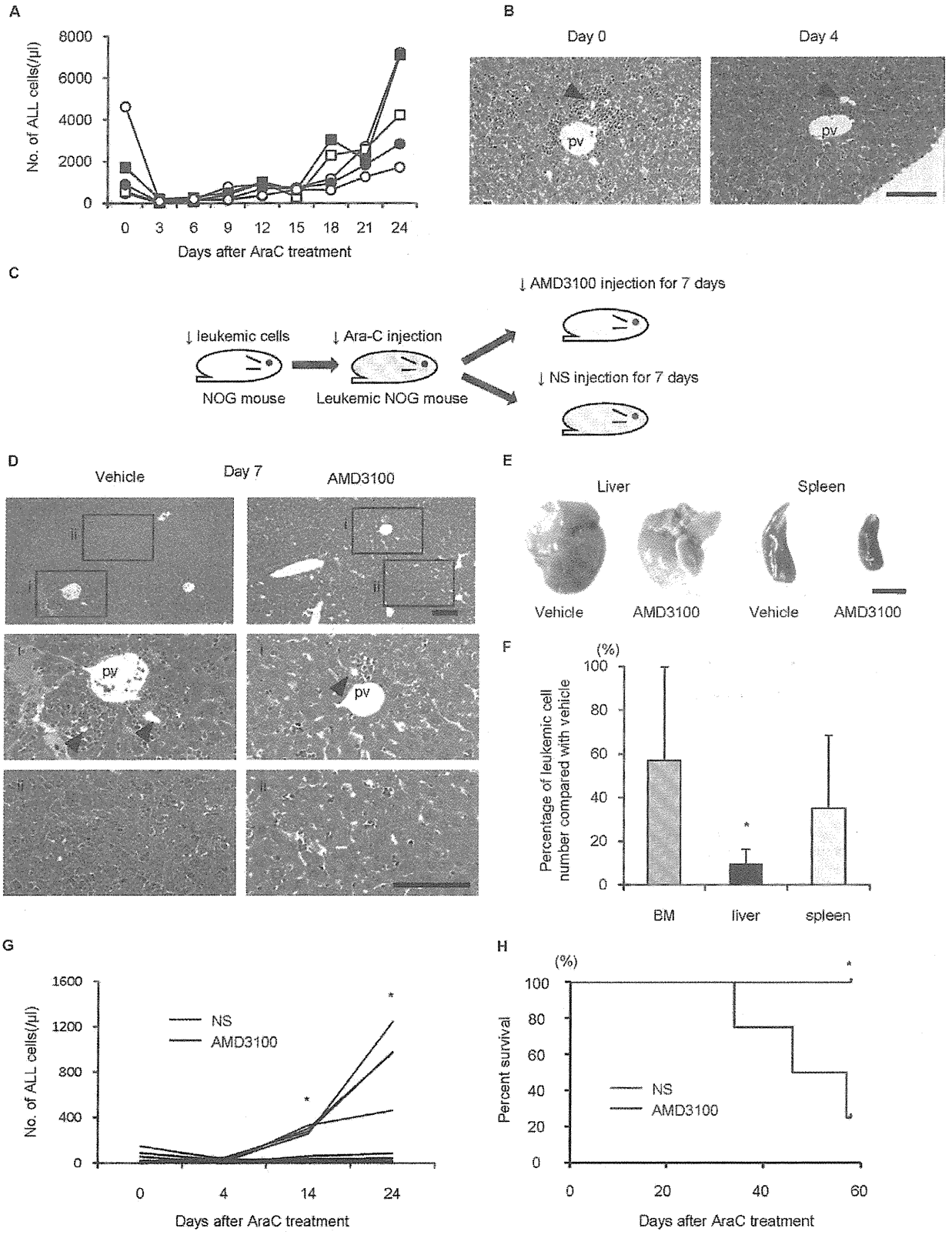
A
No. of ALL cells/(μl)
8000
6000
4000
2000
0
0 3 6 9 12 15 18 21 24
Days after AraC treatment
B
Day 0
Day 4
pv
pv
C
↓ leukemic cells
↓ Ara-C injection
NOG mouse
Leukemic NOG mouse
↓ AMD3100 injection for 7 days
↓ NS injection for 7 days
D
Vehicle
Day 7
AMD3100
pv
pv
E
Liver
Spleen
Vehicle
AMD3100
Vehicle
AMD3100
F
(%)
Percentage of leukemic cell number compared with vehicle
100
80
60
40
20
0
*
BM
liver
spleen
G
No. of ALL cells/(μl)
1600
1200
800
400
0
NS
AMD3100
*
*
0 4 14 24
Days after AraC treatment
H
(%)
Percent survival
100
80
60
40
20
0
*
NS
AMD3100
0 20 40 60
Days after AraC treatment

Figure 6. AMD3100 inhibited the *in vivo* dissemination of leukemic cells surrounding the bile ducts after chemotherapy, thus leading to the superior survival of h-leukemic NOG mice. (A) Ara-C was administered i.p. to leukemic mice, and leukemic cell counts per μl PB were monitored every three days. (B) H–E staining of leukemic liver sections before (day 0, left panel) and after (day 4, right panel) Ara-C treatment. Scale bar, 100 μm (C) Schematic of AMD3100 and normal saline (NS) injection for leukemic mice following Ara-C treatment. (D) Administration of AMD3100 resulted in reduction of leukemic cell cluster regrowth in portal areas compared with administration of NS (i).A few leukemic cells observed in the sinusoidal area in both groups (ii). pv; portal vein. Arrowheads indicate bile ducts. Scale bar, 100 μm. (E) Representative macroscopic appearance of liver and spleen in leukemic mice after AMD3100 administration. Vehicle alone group is on the left-hand side and AMD3100 injected group is on the right-hand side. Scale bar, 1 cm. (F) Percentage of leukemic cells in the BM, liver and spleen of AMD3100-treated leukemic mice compared with that of control mice. Average number of leukemic cells harvested from each organ of vehicle-injected mice was set as 100 ($*P = 0.039$, Student's *t* -test, compared with BM, $n = 5$ per condition).Data are shown as mean± S.D. (G) AMD3100 or NS was administered for up to 60 days to h-leukemic NOG mice after chemotherapy. The leukemic cell counts in the PB were monitored every ten days beginning 4 days after the chemotherapy. AMD3100 after chemotherapy prevented the recurrence of leukemia *in vivo* ($P<0.01$ on days 14 and 24). (H) The AMD3100-treated mice (n = 5) demonstrated a higher overall survival than the control mice receiving NS (n = 4), as estimated by the Kaplan-Meier method ($P = 0.0221$ for comparisons of the h-leukemic NOG mice treated with AMD3100 and NS).
doi:10.1371/journal.pone.0027042.g006

inhibited in the portal area (Figure 6D, right panel). As a result, the macroscopic size of the liver and spleen in AMD3100-treated leukemic mice was smaller than that in control mice (Figure 6E), and leukemic cell counts and organ volumes of the liver and spleen were significantly reduced (Figure S6). Interestingly, the largest decrease in leukemic cell count was observed in the liver of AMD3100-treated mice (Figure 6F), and was seemingly correlated to the frequency of CXCR4-positive leukemic cells in each organ (see Figure 4A). During the long-term administration of AMD3100 or NS up to 60 days after AraC treatment, significantly fewer leukemic cells were present in the PB of AMD3100-treated mice compared with control mice receiving NS (Figure 6G). Consequently, the control mice lost a significant amount of body weight, while the body weight of the AMD3100-treated mice was not significantly different compared with that of normal NOG mice (Figure S7). Furthermore, the AMD3100-treated mice demonstrated a higher overall survival, as estimated by the Kaplan-Meier method (Figure 6H).

Overall, these results strongly indicate that the SDF-1/CXCR4 signaling pathway plays a crucial role in re-expansion of ALL leukemic cells in the hepatic niche after chemotherapy and provide a novel anti-leukemic therapy that targets the extramedullary microenvironment.

Discussion

In this paper, we propose that leukemic extramedullary pathology is due to not only migrating, but also resident proliferating leukemic cells in the extramedullary niche. Using xeno-transplantation model, previous reports showed that human leukemic cells infiltrate the liver [13,14]; however, those reports lacked pathological or molecular assessment. Here, through the analysis of h-leukemic NOG model, we have demonstrated that hepatic extramedullary microenvironments provide a niche which harbors and propagates leukemic cells.

We also demonstrated that the SDF-1/CXCR4 axis plays a crucial role in causing liver pathology. Recent studies revealed SDF-1/CXCR4 axis involvement in the development and metastasis of solid tumor [18,19]. This axis has also been known to play an indispensable role in the homing, proliferation, and survival of both normal hematopoietic and leukemic cells in the BM niche [18,29,30,31,32,33,34,35]. In pediatric ALL patients, high expression of CXCR4 in leukemic cells was strongly predictive of extramedullary organ involvement [34], which is compatible with the findings in our murine xeno-transplantation model. By analyzing the detailed structure of the hepatic niche, we found that certain extramedullary niche was also dependent on SDF-1/CXCR4 axis for recruitment and proliferation of leukemic cells.

We showed that leukemic cells in the peripheral blood were predominantly non-proliferating, although the BM and liver contain a large proportion of proliferating leukemic cells. These findings indicate that leukemic cells can proliferate efficiently in medullary/extramedullary sites if proper microenviromental conditions are provided, but cannot in the peripheral blood where microenviromental structure is absent. This finding is also compatible with the observation that *in vitro* cultures of lymphoblastic leukemic cells are more difficult to achieve in floating conditions, like in peripheral blood, than on stromal cell layers, like cells in medullary/extramedullary microenvironment [36].

In our therapeutic model, AMD3100 prevented extramedullary regrowth of leukemic cells after chemotherapy and dramatically improved the overall survival. Importantly, without AMD3100 administration, a few leukemic cells remaining in the portal region after chemotherapy appeared to contributed to the regrowth of leukemia. We speculate that two reasons may account for this extramedullary regrowth of leukemic cells. First, chemotherapy resistance may be induced by epithelial cells in the portal areas. In the BM, direct contact between ALL leukemic cells and stromal cells is one of the important mechanisms to induce drug resistance for leukemic cells [25]. Thus, it is very likely that leukemic cells next to hepatic niche cells can survive chemotherapy in an analogous manner. Second, a more fundamental reason is derived from the concept of the leukemic stem cells which have potency to regenerate leukemia [37] and contribute to relapse [5]. In acute myeloid leukemia (AML) in the BM, CD34-positive leukemic stem cells contribute to AML relapse by homing in on and expanding within the niche usually occupied by normal hematopoietic stem cells [5]. Furthermore, it has recently been shown that Ara-C treatment specifically targeted proliferating cells in an AML xenograft model, resulting in the enrichment of quiescent leukemic stem cells in the G0/G1 phase of the cell cycle, thereby contributing to disease relapse [38]. Our current data also showed that quiescent clones were not affected by chemotherapy, and thereby subsequently contribute to disease recurrence. Interestingly, during liver regeneration, the portal area serves as an important niche for both oval cells and migrating hematopoietic stem cells [10,15,39]. If ALL cells arise via a leukemic stem cell hierarchy similar to AML [37], this hepatic niche may serve as a haven for leukemic stem cell survival and proliferation. Considering the aforementioned reasons for the persistent presence of leukemic cells, extramedullary niche-targeting therapy could be a powerful option for preventing recurrence in extramedullary organs as well as the BM.

In conclusion, using the h-leukemic NOG model, we demonstrated that the extramedullary dissemination of leukemia is not due to nonselective infiltration, but rather systematic invasion and proliferation of leukemic cells in a particular niche at extramedullary sites. Because various signals from the leukemic niche may contribute to the progression of leukemia, future studies that

elucidate the complexity of leukemic cell-host interactions will be necessary for developing novel niche-targeted therapeutics.

Materials and Methods

Mice

NOG mice were developed at the Central Institute of Experimental Animals (Kawasaki, Japan), as previously described[9]. All mice were kept under specific pathogen-free conditions in accordance with the guidelines of the facility.

Human samples

BM samples were collected from patients with pediatric ALL at the time of diagnosis with written informed consent under the guidelines of the institutional ethics committee, Kyoto University Graduate School and Faculty of Medicine, Ethics Committee (approval ID is G-283). Mononuclear cells were separated by Ficoll-Hypaque density gradient centrifugation soon after aspiration.

Primary and serial xenogeneic transplantation of ALL cells into NOG mice

Xeno-transplantation and analysis of ALL cells were performed by modifying previously reported methods[8]. In brief, leukemic cells (1×10^6cells) were transplanted into non-pretreated 8- to 10-week old NOG mice by the tail vein or via intra-femoral injection. For serial transplantation, leukemic cells were obtained from the recipient BM and intravenously transplanted into non-pretreated NOG mice via the tail vein.

Flow cytometric analysis of mice with transplanted leukemic cells

For analysis of leukemic cells in organs, mice were sacrificed by cervical dislocation at the indicated times after transplantation. After as much peripheral blood was collected as possible, the BM, liver and spleen were removed and mechanically dispersed. Samples from each organ were stained with antibodies after isolation of mononuclear cells. Dead cells were excluded by 4′-6-Diamidino-2-phenylindole (DAPI) staining. Samples were analyzed using a FACS LSR and Cell Quest software (Becton Dickinson) according to the manufacturer's protocol. Antibodies used for flow cytometric analysis were anti-human CD45-allophycocyanin (APC) (BD Pharmingen), anti-human N-CAM-APC (BD Pharmingen), anti-mouse CD45-APC (BD Pharmingen), anti-human CD19-phycoerythrin (PE) (eBiosciences), anti-human CXCR4-PE (BD Pharmingen), anti-human CD44-PE (BD Pharmingen), anti-human very late antigen-4 (VLA-4)-PE (BD Pharmingen), anti-human CC chemokine receptor 7 (CCR7)-PE (R&D Systems), anti-human CD45-fluorescein isothiocyanate (FITC) (BD Biosciences), and anti-human CD19-FITC (Dako).

Histological analysis of patient and mouse samples

The histological analysis of patient samples and mouse BM was performed by May-Grunwald Giemsa staining of cytospine preparations using standard procedures. Hematoxylin-Eosin (H-E) staining was performed on tissue sections derived from the recipient mice. Detection of human leukemic cells in the murine organs by immunohistochemical analysis was performed using a previously reported method[10]. The antibodies (and dilutions) used were mouse anti-human CD45 (1:100) (DAKO), mouse anti-human/mouse CXCL12/SDF-1α antibody (1:100) (R&D Systems), rabbit polyclonal CXCR4 (Abcam) and Cy3-conjugated donkey anti-mouse IgG or FITC-conjugated donkey anti-rabbit IgG at a dilution of 1:100 (both from Jackson ImmunoResearch Laboratories). Hoechst 33324 (Invitrogen) was used for nuclear staining. Prepared samples were then examined under a light or fluorescence microscope (Olympus).

5-bromo-2-deoxyuridine (BrdU) staining

In vivo BrdU labeling was performed by injecting leukemic mice with 0.2 ml BrdU (5 mg/ml, Sigma) intraperitoneally three times at 4, 24, and 48 h before analysis. Immunohistochemical staining of BrdU was performed using a BrdU staining kit (Invitrogen) according to the manufacturer's protocol.

Cell cycle analysis

For quantification of cells in the S/G2/M phase of the cell cycle, ALL-engrafted recipient BM, peripheral blood, and liver oriented leukemia cells were labeled with Hoechst 33342 and pyronin Y, or Propidium Iodide (PI) using standard procedures. Samples were analyzed using FACS LSR and Cell Quest software (Becton Dickinson).

Migration assay

A total of 5×10^5 cells in a volume of 0.5 mL were added to the top chamber of 24 well MULTIWELL™ plates (Becton Dickinson). The wells separate cells using a polycarbonate membrane filter (3.0 μm pore size) from a lower compartment containing 0.5 mL RPMI with 10% FCS containing 250 ng/ml SDF-1α (R&D Systems). Chemotaxis assays were conducted at 37°C for 4 h. Some assays were performed using leukemic cells preincubated for 30 min at 37°C in the presence of AMD3100 (0.1 mg/ml) (Sigma).

Colony assays

Colony assays were performed by modifying a previously reported method[40]. Leukemic cells were incubated in a methylcellulose culture dish at a concentration of 1×10^6 cells/mL. Some experiments were performed on leukemic cells preincubated for 30 min at 37°C in the presence of AMD3100 (0.1 mg/ml) before the colony assays. SDF-1α (R&D Systems) was added to the control cytokines at a concentration of 250 ng/ml. Colonies were harvested, washed twice and cytospine stained with May-Grunwald Giemsa stains to identify leukemic cells.

Western blot analysis

A total of 5×10^5 leukemic cells were pretreated for 30 min at 37°C in the presence or absence of AMD3100 (0.1 mg/ml) and then incubated with or without 100 ng/mL SDF-1α for 5 minute. After that, cells were lysed in ice-cold lysis buffer (Thermo Scientific) supplemented with a protease inhibitor cocktail (Nacalai tesque). Lysates were then separated on a 10% polyacrylamide gel, transferred to Immobilon-P membranes (Millipore), probed with the appropriate antibodies (anti–human AKT, Ser 473–phosphorylated AKT, ERK, phosphorylated ERK , β-Actin from Cell Signaling Technologies), and visualized using an enhanced chemiluminescence (ECL) plus kit (GE Healthcare).

Cytosine arabinoside (Ara-C) treatment and AMD3100 administration

Intraperitoneal (i.p.) injection of 75 mg/kg Ara-C (Sigma) was performed in NOG recipients transplanted with leukemic cells. AMD3100 (Sigma) was administered intraperitoneally at a dose of 200 μg for 7 days or up to 60 days in the long-term assay starting the day after Ara-C injection.

Statistical analysis

Statistical comparisons between experimental groups were analyzed using the Student's *t*-test or paired *t*-test, and for all comparisons a *P* value less than .05 was considered significant.

Supporting Information

Figure S1 NOG mice support efficient human primary ALL engraftment without pre-conditioning. Primary human ALL engraftment in NOG mice injected with 1×10^6 BMMNCs from nine ALL patients. Percentage of human ALL cells (hCD45+ or hCD19+ cells) in recipient BM determined one to five months post-injection. Numbers in circles indicate case number and show mean percentage of ALL cells in recipient BM in each cases ($n=1-6$ mice per case).
(TIF)

Figure S2 BM, liver and spleen contain plenty of leukemic cells. Pale BM, enlarged liver and spleen were massively infiltrated with leukemic cells. Histologically, no specific sites of infiltration were observed in the spleens of the transplanted NOG mice. Scale bar, 50 μm.
(TIFF)

Figure S3 The actual interaction between CXCR4 on leukemic cells and SDF1. Representative images of Proximity Ligation Analysis (PLA) detected by the Duolink Detection kit (Olink Bioscience, Uppsala, Sweden). The system elicits a visible signal only when the two antibodies (i.e. anti-SDF-1 and anti-CXCR4) are in close proximity. Arrows denote regions of signal amplification indicating the actual interaction between SDF-1 and CXCR4. Nuclear stain is DAPI (Blue). Scale bar indicates 50 μm.
(TIF)

Figure S4 The checker board assay. Increasing concentrations of SDF-1α were added to upper or lower compartments of migration chambers. Significant increases in numbers of migrating cells were observed when reagent was added to lower chambers. Baseline was defined as result of assay without SDF-1α. Increasing concentrations of SDF-1α were added to upper or lower compartments of migration chambers. Significant increases in numbers of migrating cells were observed when reagent was added to lower chambers. Baseline was defined as result of assay without SDF-1α.
(TIF)

Figure S5 AraC preferentially eliminates cycling leukemic cells *in vivo*. The cell cycle analysis of leukemic cells harvested from the liver before and after AraC treatment (80 mg/mice). The liver-oriented leukemic cells in the G2/M-phase of the cell cycle were preferentially eliminated, and the quiescent clones were not affected by the chemotherapy.
(TIF)

Figure S6 AMD3100 inhibits hepatosplenomegaly. Leukemic cell numbers (A) and weights of livers and spleens (B) from leukemic mice treated with vehicle alone (saline) or AMD3100 after Ara-C treatment. Each graph shows mean cell numbers and weights (* $P<0.05$. Student's *t*- test, $n=5$ per condition). Data are shown as means±S.D.
(TIF)

Figure S7 Administration of AMD3100 after chemotherapy prevented the recurrence of leukemia *in vivo*. Control mice receiving NS experienced relapsed leukemia and lost significant body weight compared with AMD3100-treated mice ($P<0.01$. Student's *t*- test, $n=4-5$ per condition) and age-matched normal NOG mice ($P<0.01$). On the other hand, the body weight of the AMD3100-treated mice was not significantly different in comparison to that of the age-matched normal NOG mice.
(TIF)

Acknowledgments

We thank the ALL patients who participated in this study. We are grateful to Dr. S.Teramukai (Kyoto University, Kyoto, Japan) for statistical analysis, Dr. A.Tsuchiya (Niigata University, Niigata, Japan) for critical suggestions, and Teddy Kamata (University of Oxford, Oxford, United Kingdom) for manuscript editing.

Author Contributions

Conceived and designed the experiments: AN TH FI TN. Performed the experiments: IK MM YN. Analyzed the data: IK AN TH HF MKS KU HH FI TN. Contributed reagents/materials/analysis tools: MI SA. Wrote the paper: IK.

References

1. Pui CH, Evans WE (2006) Treatment of acute lymphoblastic leukemia. N Engl J Med 354: 166–178.
2. Pui CH, Robison LL, Look AT (2008) Acute lymphoblastic leukaemia. Lancet 371: 1030–1043.
3. Einsiedel HG, von Stackelberg A, Hartmann R, Fengler R, Schrappe M, et al. (2005) Long-term outcome in children with relapsed ALL by risk-stratified salvage therapy: results of trial acute lymphoblastic leukemia-relapse study of the Berlin-Frankfurt-Munster Group 87. J Clin Oncol 23: 7942–7950.
4. Iwamoto S, Mihara K, Downing JR, Pui CH, Campana D (2007) Mesenchymal cells regulate the response of acute lymphoblastic leukemia cells to asparaginase. J Clin Invest 117: 1049–1057.
5. Ishikawa F, Yoshida S, Saito Y, Hijikata A, Kitamura H, et al. (2007) Chemotherapy-resistant human AML stem cells home to and engraft within the bone-marrow endosteal region. Nat Biotechnol 25: 1315–1321.
6. Kucia M, Jankowski K, Reca R, Wysoczynski M, Bandura L, et al. (2004) CXCR4-SDF-1 signalling, locomotion, chemotaxis and adhesion. J Mol Histol 35: 233–245.
7. Winick NJ, Smith SD, Shuster J, Lauer S, Wharam MD, et al. (1993) Treatment of CNS relapse in children with acute lymphoblastic leukemia: A Pediatric Oncology Group study. J Clin Oncol 11: 271–278.
8. Hiramatsu H, Nishikomori R, Heike T, Ito M, Kobayashi K, et al. (2003) Complete reconstitution of human lymphocytes from cord blood CD34+ cells using the NOD/SCID/gammacnull mice model. Blood 102: 873–880.
9. Ito M, Hiramatsu H, Kobayashi K, Suzue K, Kawahata M, et al. (2002) NOD/SCID/gamma(c)(null) mouse: an excellent recipient mouse model for engraftment of human cells. Blood 100: 3175–3182.
10. Fujino H, Hiramatsu H, Tsuchiya A, Niwa A, Noma H, et al. (2007) Human cord blood CD34+ cells develop into hepatocytes in the livers of NOD/SCID/gamma(c)null mice through cell fusion. FASEB J 21: 3499–3510.
11. Kambe N, Hiramatsu H, Shimonaka M, Fujino H, Nishikomori R, et al. (2004) Development of both human connective tissue-type and mucosal-type mast cells in mice from hematopoietic stem cells with identical distribution pattern to human body. Blood 103: 860–867.
12. Kato M, Sanada M, Kato I, Sato Y, Takita J, et al. (2009) Frequent inactivation of A20 in B-cell lymphomas. Nature 459: 712–716.
13. Lock RB, Liem N, Farnsworth ML, Milross CG, Xue C, et al. (2002) The nonobese diabetic/severe combined immunodeficient (NOD/SCID) mouse model of childhood acute lymphoblastic leukemia reveals intrinsic differences in biologic characteristics at diagnosis and relapse. Blood 99: 4100–4108.
14. Kong Y, Yoshida S, Saito Y, Doi T, Nagatoshi Y, et al. (2008) CD34+CD38+CD19+ as well as CD34+CD38-CD19+ cells are leukemia-initiating cells with self-renewal capacity in human B-precursor ALL. Leukemia 22: 1207–1213.
15. Kollet O, Shivtiel S, Chen YQ, Suriawinata J, Thung SN, et al. (2003) HGF, SDF-1, and MMP-9 are involved in stress-induced human CD34+ stem cell recruitment to the liver. J Clin Invest 112: 160–169.

16. Reiter A, Schrappe M, Ludwig WD, Hiddemann W, Sauter S, et al. (1994) Chemotherapy in 998 unselected childhood acute lymphoblastic leukemia patients. Results and conclusions of the multicenter trial ALL-BFM 86. Blood 84: 3122–3133.
17. Alastair D, Burt BCP, Linda DFerrell (2007) MacSween's Pathology of the Liver. 992 p.
18. Muller A, Homey B, Soto H, Ge N, Catron D, et al. (2001) Involvement of chemokine receptors in breast cancer metastasis. Nature 410: 50–56.
19. Libura J, Drukala J, Majka M, Tomescu O, Navenot JM, et al. (2002) CXCR4-SDF-1 signaling is active in rhabdomyosarcoma cells and regulates locomotion, chemotaxis, and adhesion. Blood 100: 2597–2606.
20. Zeng Z, Shi YX, Samudio IJ, Wang RY, Ling X, et al. (2009) Targeting the leukemia microenvironment by CXCR4 inhibition overcomes resistance to kinase inhibitors and chemotherapy in AML. Blood 113: 6215–6224.
21. Jin L, Hope KJ, Zhai Q, Smadja-Joffe F, Dick JE (2006) Targeting of CD44 eradicates human acute myeloid leukemic stem cells. Nat Med 12: 1167–1174.
22. Buonamici S, Trimarchi T, Ruocco MG, Reavie L, Cathelin S, et al. (2009) CCR7 signalling as an essential regulator of CNS infiltration in T-cell leukaemia. Nature 459: 1000–1004.
23. Chang H, Brandwein J, Yi QL, Chun K, Patterson B, et al. (2004) Extramedullary infiltrates of AML are associated with CD56 expression, 11q23 abnormalities and inferior clinical outcome. Leuk Res 28: 1007–1011.
24. Matsunaga T, Takemoto N, Sato T, Takimoto R, Tanaka I, et al. (2003) Interaction between leukemic-cell VLA-4 and stromal fibronectin is a decisive factor for minimal residual disease of acute myelogenous leukemia. Nat Med 9: 1158–1165.
25. Mudry RE, Fortney JE, York T, Hall BM, Gibson LF (2000) Stromal cells regulate survival of B-lineage leukemic cells during chemotherapy. Blood 96: 1926–1932.
26. Kawaguchi A, Orba Y, Kimura T, Iha H, Ogata M, et al. (2009) Inhibition of the SDF-1alpha-CXCR4 axis by the CXCR4 antagonist AMD3100 suppresses the migration of cultured cells from ATL patients and murine lymphoblastoid cells from HTLV-I Tax transgenic mice. Blood 114: 2961–2968.
27. Coulomb-L'Hermin A, Amara A, Schiff C, Durand-Gasselin I, Foussat A, et al. (1999) Stromal cell-derived factor 1 (SDF-1) and antenatal human B cell lymphopoiesis: expression of SDF-1 by mesothelial cells and biliary ductal plate epithelial cells. Proc Natl Acad Sci U S A 96: 8585–8590.
28. Nagasawa T, Hirota S, Tachibana K, Takakura N, Nishikawa S, et al. (1996) Defects of B-cell lymphopoiesis and bone-marrow myelopoiesis in mice lacking the CXC chemokine PBSF/SDF-1. Nature 382: 635–638.
29. Juarez J, Baraz R, Gaundar S, Bradstock K, Bendall L (2007) Interaction of interleukin-7 and interleukin-3 with the CXCL12-induced proliferation of B-cell progenitor acute lymphoblastic leukemia. Haematologica 92: 450–459.
30. Lee Y, Gotoh A, Kwon HJ, You M, Kohli L, et al. (2002) Enhancement of intracellular signaling associated with hematopoietic progenitor cell survival in response to SDF-1/CXCL12 in synergy with other cytokines. Blood 99: 4307–4317.
31. Ara T, Tokoyoda K, Sugiyama T, Egawa T, Kawabata K, et al. (2003) Long-term hematopoietic stem cells require stromal cell-derived factor-1 for colonizing bone marrow during ontogeny. Immunity 19: 257–267.
32. Lataillade JJ, Clay D, Dupuy C, Rigal S, Jasmin C, et al. (2000) Chemokine SDF-1 enhances circulating CD34(+) cell proliferation in synergy with cytokines: possible role in progenitor survival. Blood 95: 756–768.
33. Spiegel A, Kollet O, Peled A, Abel L, Nagler A, et al. (2004) Unique SDF-1-induced activation of human precursor-B ALL cells as a result of altered CXCR4 expression and signaling. Blood 103: 2900–2907.
34. Crazzolara R, Kreczy A, Mann G, Heitger A, Eibl G, et al. (2001) High expression of the chemokine receptor CXCR4 predicts extramedullary organ infiltration in childhood acute lymphoblastic leukaemia. Br J Haematol 115: 545–553.
35. Juarez J, Dela Pena A, Baraz R, Hewson J, Khoo M, et al. (2007) CXCR4 antagonists mobilize childhood acute lymphoblastic leukemia cells into the peripheral blood and inhibit engraftment. Leukemia 21: 1249–1257.
36. Manabe A, Murti KG, Coustan-Smith E, Kumagai M, Behm FG, et al. (1994) Adhesion-dependent survival of normal and leukemic human B lymphoblasts on bone marrow stromal cells. Blood 83: 758–766.
37. Bonnet D, Dick JE (1997) Human acute myeloid leukemia is organized as a hierarchy that originates from a primitive hematopoietic cell. Nat Med 3: 730–737.
38. Saito Y, Uchida N, Tanaka S, Suzuki N, Tomizawa-Murasawa M, et al. (2010) Induction of cell cycle entry eliminates human leukemia stem cells in a mouse model of AML. Nat Biotechnol 28: 275–280.
39. Kuwahara R, Kofman AV, Landis CS, Swenson ES, Barendswaard E, et al. (2008) The hepatic stem cell niche: identification by label-retaining cell assay. Hepatology 47: 1994–2002.
40. Ueda T, Tsuji K, Yoshino H, Ebihara Y, Yagasaki H, et al. (2000) Expansion of human NOD/SCID-repopulating cells by stem cell factor, Flk2/Flt3 ligand, thrombopoietin, IL-6, and soluble IL-6 receptor. J Clin Invest 105: 1013–1021.

Cancer Science
The official journal of the Japanese Cancer Association JCA

Mismatched human leukocyte antigen class II-restricted CD8$^+$ cytotoxic T cells may mediate selective graft-versus-leukemia effects following allogeneic hematopoietic cell transplantation

Tomoya Hirosawa,[1,2,9] Hiroki Torikai,[1,9] Mayumi Yanagisawa,[3] Michi Kamei,[1] Nobuhiko Imahashi,[3] Ayako Demachi-Okamura,[1] Miyoko Tanimoto,[1] Keiko Shiraishi,[1] Mamoru Ito,[4] Koichi Miyamura,[3] Kiyosumi Shibata,[2] Fumitaka Kikkawa,[2] Yasuo Morishima,[5] Toshitada Takahashi,[6] Nobuhiko Emi,[7] Kiyotaka Kuzushima[1] and Yoshiki Akatsuka[1,7,8]

[1]Division of Immunology, Aichi Cancer Center Research Institute, Nagoya; [2]Department of Obstetrics and Gynecology, Nagoya University Graduate School of Medicine, Nagoya; [3]Department of Hematology, Japanese Red Cross Nagoya First Hospital, Nagoya; [4]Central Institute for Experimental Animals, Kanagawa; [5]Department of Hematology and Chemotherapy, Aichi Cancer Center Research Institute, Nagoya; [6]Comprehensive Health Science Center, Higashiwura; [7]Department of Hematology, Fujita Health University, Toyoake, Japan

(Received January 25, 2011/Revised March 22, 2011/Accepted March 27, 2011/Accepted manuscript online April 5, 2011/Article first published online May 9, 2011)

Partial human leukocyte antigen (HLA)-mismatched hematopoietic stem cell transplantation (HSCT) is often performed when an HLA-matched donor is not available. In these cases, CD8$^+$ or CD4$^+$ T cell responses are induced depending on the mismatched HLA class I or II allele(s). Herein, we report on an HLA-DRB1*08:03-restricted CD8$^+$ CTL clone, named CTL-1H8, isolated from a patient following an HLA-DR-mismatched HSCT from his brother. Lysis of a patient Epstein–Barr virus-transformed B cell line (B-LCL) by CTL-1H8 was inhibited after the addition of blocking antibodies against HLA-DR and CD8, whereas antibodies against pan-HLA class I or CD4 had no effect. The 1H8-CTL clone did not lyse the recipient dermal fibroblasts whose HLA-DRB1*08:03 expression was upregulated after 1 week cytokine treatment. Engraftment of HLA-DRB1*08:03-positive primary leukemic stem cells in non-obese diabetic/severe combined immunodeficient/γc-null (NOG) mice was completely inhibited by the *in vitro* preincubation of cells with CTL-1H8, suggesting that HLA-DRB1*08:03 is expressed on leukemic stem cells. Finally, analysis of the precursor frequency of CD8$^+$ CTL specific for recipient antigens in post-HSCT peripheral blood T cells revealed a significant fraction of the total donor CTL responses towards the individual mismatched HLA-DR antigen in two patients. These findings underscore unexpectedly significant CD8 T cell responses in the context of HLA class II. (*Cancer Sci* 2011; 102: 1281–1286)

Allogeneic hematopoietic stem cell transplantation (HSCT) has been used successfully for the treatment of hematological malignancies. Although HSCT from human leukocyte antigen (HLA)-identical siblings or unrelated donors is feasible to minimize the risk of acute graft-versus-host disease (aGVHD), HSCT from HLA-mismatched donors can be performed when a patient has advanced disease and no HLA matched donor is available.[1] It has been shown that aGVHD and survival rates are comparable between patients receiving HLA-mismatched unrelated HSCT and those receiving fully HLA-matched HSCT when the mismatch combination is not non-permissive.[2] Because the mismatched HLA molecule(s) may serve as a target for donor T cells, the immune response to these HLA in patients receiving a zero non-permissible mismatch HSCT could give rise to a favorable graft-versus-leukemia (GVL) effect with minimal risk of aGVHD. Following HLA-mismatched HSCT, it is commonly believed that CD8$^+$ or CD4$^+$ T cell responses are induced, depending on the mismatched HLA class I or II allele(s), based on the binding of cognate coreceptors to MHC molecules stabilizing weak interactions between T cell receptors (TCR) and MHC.[3]

In the present study, we characterized an HLA class II-restricted CTL clone isolated from a patient with acute myeloid leukemia who received HLA-DR/DP loci-mismatched HSCT. The CTL clone, named CTL-1H8, was CD8$^+$ and its cytotoxicity was blocked by an anti-CD8 antibody as well as by an anti-HLA-DR antibody. The CTL-1H8 clone lysed primary leukemic cells possessing the mismatched HLA-DRB1*08:03, but not cytokine-treated recipient dermal fibroblasts. Engraftment of HLA-DRB1*08:03-positive primary leukemic stem cells in immunodeficient mice[4] was completely inhibited by *in vitro* preincubation with CTL-1H8. Furthermore, we demonstrated by CTL precursor (CTLp) frequency analysis that a significant fraction of the total donor CD8$^+$ CTL response in this patient was directed against the HLA-DRB1*08:03 molecule. These findings underscore the *in vivo* immunological relevance of a CD8$^+$ T cell response against mismatched HLA class II molecule(s).

Materials and Methods

Cells, HLA transfectants, and antibodies. Peripheral blood mononuclear cells (PBMC) were collected and cryopreserved before and after HSCT from a male patient who had received his brother's bone marrow (BM) for AML (M6; French American British subtype, M6). The HLA genotype of the recipient was A*24:02/*33:03, B*52:01/*44:03, C*12:02/*14:03, DRB1*08:03/*13:02, DQB1*06:01/*06:04, DPB1*02:02/*04:01, whereas that of the donor was mismatched by DRB1*15:02 instead of DRB1*08:03 and by DPB1*05:01 instead of DPB1*02:02. The patient developed grade II aGVHD limited to the skin and extensive chronic GVHD, but has been free from disease recurrence for over 2 years. B-Lymphoblastoid cell lines (B-LCL) were established from the donor and recipient, as well as from normal volunteers. All blood, BM, and tissue samples were collected after the subjects had provided written informed consent, and the study was approved by the Institutional Review Board of Aichi Cancer Center. The B-LCL, including the HLA class I negative B-LCL line 721.221, were

[8]To whom correspondence should be addressed.
E-mail: yos-akatsuk@umin.ac.jp
[9]These authors contributed equally to the study.

doi: 10.1111/j.1349-7006.2011.01949.x

maintained in RPMI 1640 medium supplemented with 10% FCS (Immuno-Biological Laboratory, Gunma, Japan), 2 mM L-glutamine, and penicillin/streptomycin (referred to as ''culture medium''). The B-LCL were transduced with retroviral vectors carrying individual HLA class I or class II cDNAs, as described previously.[5] The mAbs used in the present study were against the following antigens: pan HLA class I, HLA-DR, HLA-DQ, HLA-DP, CD4, CD8, CD45, and CD34 (all from BD Biosciences, Franklin Lakes, NJ, USA); HLA-DR8 (One Lambda, Canoga Park, CA, USA); and FITC-conjugated rabbit anti-mouse IgM (BD Biosciences). The mAb blocking experiments were performed using final concentrations of 20 μg/mL mAb. Stained cells were analyzed with a FACSCalibur flow cytometer and CellQuest software (BD Biosciences).

Generation of CTL lines and clones. The CTL lines were generated from the $CD8^+$ fraction of post-HSCT PBMC after three stimulations with irradiated (33 Gy) pre-HSCT recipient PBMC. Interleukin (IL)-2 (20 U/mL; Chiron, Emeryville, CA, USA) was added on Days 1 and 5 after the second and third stimulation. The CTL clones were generated by limiting dilution and expanded as described previously[6,7] and were frozen until use. All cultures were performed in RPMI 1640 medium supplemented with 4% pooled human serum, 2 mM L-glutamine, and penicillin/streptomycin (referred to as ''CTL medium'').

Purification of $CD34^+$ leukemia cells using magnetic beads. Primary leukemic cells carrying HLA-DRB1*08:03 that had been collected and cryopreserved at the time of diagnosis were thawed and positively selected for $CD34^+$ subsets using phycoerythrine (PE)-conjugated anti-CD34 mAb (BD Biosciences) and anti-PE immunomagnetic beads through MACS MS columns (Miltenyi Biotec, Bergisch Gladbach, Germany).

Cytotoxicity assays. Target cells were radiolabelled with 3.7 MBq ^{51}Cr for 2 h and 1×10^3 target cells/well were mixed with CTL at various effector/target (E/T) ratios in a standard 4-h cytotoxicity assay using 96-well round-bottomed plates. All assays were performed at least in duplicate. Primary dermal fibroblasts from the skin were treated with interferon (IFN)-γ (100 U/mL; Endogen, Woburn, MA, USA) and tumor necrosis factor (TNF)-α (10 ng/mL; Endogen) for 48 h or 7 days, as indicated. Percentage specific lysis was calculated as follows:

(Experimental c.p.m. − Spontaneous c.p.m.)/(Maximum c.p.m. − Spontaneous c.p.m.) × 100

Leukemic stem cell engraftment assay in immunodeficient mice. Non-obese diabetic/severe combined immunodeficient/γc-null (NOG) mice[4] were purchased from the Central Institute for Experimental Animals (Kanagawa, Japan). All mice were maintained under specific pathogen-free conditions in the Aichi Cancer Center Research Institute. The Ethics Review Committee of the Institute approved the experimental protocol. The $CD34^+$ fraction (3.0×10^6) of Philadelphia chromosome (Ph)-positive primary acute lymphoblastic leukemia (ALL) cells was preincubated for 16 h in CTL medium supplemented with 20 units/mL IL-2 at 37°C with 5% CO_2 either alone or in the presence of CTL-1H8 or a control CTL-1B9 (HLA-A*24:02-restricted, minor histocompatibility antigen-specific CTL[8]) at a T cell:ALL cell ratio of 1:1. Thereafter, the cultures were harvested, resuspended in a total volume of 300 μL CTL medium, and inoculated via the tail vein into 8–10-week-old NOG mice. Six to 7 weeks after inoculation, mice were killed, peripheral blood was aspirated from the heart, and BM cells were obtained by flushing the femora with complete medium. Nucleated cells were analyzed for the expression of human CD45, human CD34, or HLA-DR.

Limiting dilution-based CTLp frequency assay. The proportion of CTLp specific for the HLA-DRB1*08:03 of the total CTLp against potential recipient alloantigens was quantitated using a standard limiting dilution assay. Purified $CD8^+$ T cells from the PBMC obtained on specific days after HSCT, as indicated, were cultured at twofold serial dilutions with 33 Gy-irradiated 3×10^4 CD40-activated B (CD40-B) cells generated from pre-HSCT recipient PBMC in 96-well round-bottomed plates in CTL medium.[5] On Days 2 and 5, 50 U/mL IL-2 was added after each restimulation. There were at least 12 replicates for each dilution. After three rounds of stimulation, a split-well analysis was performed for HLA-DRB1*08:03-specific cytotoxicity against ^{51}Cr-radiolabeled donor B-LCL with or without HLA-DRB1*08:03 cDNA transduction or recipient B-LCL. The wells were considered to be positive if the total c.p.m. released by the effector cells was >3 SD above that in control wells (mean c.p.m. released by the target cells incubated with irradiated stimulator cells alone). In addition, $CD8^+$ cells from another recipient receiving HLA class II-mismatched HSCT were tested in a similar way. Finally, the CTLp frequency was calculated using L-Calc software (StemCell Technologies, Vancouver, BC, Canada).[9]

Results

Cytotoxicity of the $CD8^+$ CTL clone against allogeneic HLA-DRB1*08:03-positive hematopoietic cells. In all, 27 clones cytotoxic to recipient but not donor B-LCL were isolated by limiting dilution from $CD8^+$ T cells obtained on Day 207 after HSCT. Based on HLA restriction analysis using partially HLA-matched panel B-LCL, three groups of clones were identified: the first two groups (five in group 1 and 14 in group 2) were potentially restricted by HLA-A*24:02, A*33:03, B*44:03, and C*14:03 and showed lytic activity against cytokine-treated fibroblasts; the remaining eight clones in group 3 showed no lytic activity against cytokine-treated fibroblasts and were potentially restricted by HLA-A*24:02 or C*14:02. Because our primary goal was to generate CTL clones that recognized hematopoietic cells, including leukemic cells for selective GVL effect induction,[10] we omitted the group 1 and 2 clones. Of the eight group 3 clones, we chose CTL-1H8 as a representative CTL clone for further analysis owing to its superior lytic and expansion performance.

The CTL-1H8 clone was $CD8^+$ (Fig. 1a) and efficiently lysed recipient B-LCL and phytohemagglutinin-stimulated T cell lines (PHA-blasts) but not donor LCL (Fig. 1b), indicating that CTL-1H8 recognized recipient-specific alloantigen. Surprisingly, antibody-blocking experiments revealed that lytic activity against recipient B-LCL was significantly inhibited by the addition of anti-HLA-DR mAb and anti-CD8 mAb (Fig. 1c). This led us to re-examine CTL-1H8 HLA restriction using B-LCL with or without cDNA transduction of HLA-DRB1*08:03, which was mismatched between the recipient and donor. As shown in Figure 1(d), CTL-1H8 lytic activity was observed only when donor B-LCL, irrelevant B-LCL, or 721.221 B-LCL (all HLA-DRB1*08:03 deficient) were transduced with HLA-DRB1*08:03 cDNA, indicating unexpectedly that CTL-1H8 was restricted by HLA class II molecules, which are generally thought to be recognized by $CD4^+$ T cells. Because 21.221 B-LCL was deficient for HLA class I molecules, the possibility of presentation of the HLA-DBB1*0803-derived peptides to CTL-1H8 is unlikely.

Because HLA class II expression is restricted to hematopoietic cells and a fraction of activated non-hematopoietic cells, CTL recognizing HLA class II molecules could selectively mediate the GVL effect without GVHD.[11,12] Thus, we examined whether HLA-DRB1*08:03 expression on dermal fibroblasts and their susceptibility to CTL may change before and after cytokine treatment. To this end, the recipient dermal fibroblasts were incubated with IFN-γ and TNF-α for 2 or 7 days and analyzed for HLA-DR8 expression with a DR8-specific mAb. As shown in Figure 2(a), cytokine treatment for 2 days did not induce HLA-DR8 expression at all, whereas 7 days of treatment

doi: 10.1111/j.1349-7006.2011.01949.x

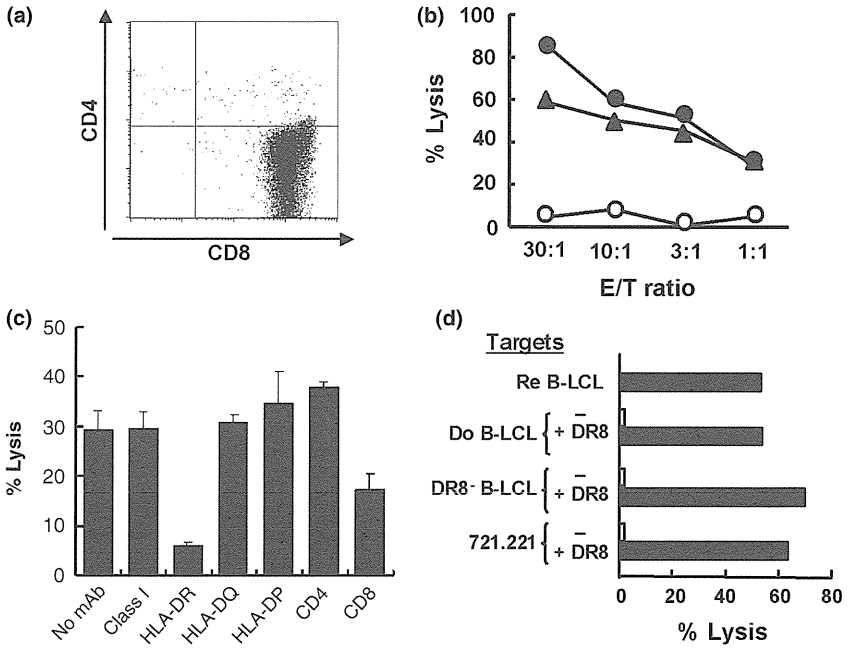

Fig. 1. Characteristics of the human leukocyte antigen (HLA)-DR8-restricted CTL clone, 1H8. (a) The cytolytic activity of CTL-1H8 was evaluated in a standard 4-h ^{51}Cr release assay. The recognition by CTL-1H8 of target cells was examined against B-lymphoblastoid cell lines (B-LCL) derived from the recipient (Re) and donor (Do), and phytohemagglutinin-stimulated T cell lines (PHA blasts). (b) Flow cytometric analysis of CTL-1H8 for CD4 and CD8. (●), Re B-LCL; (○), Do B-LCL; (▲), Re PHA blasts. (c) Antibody blocking of cytolysis was performed at an effector/target (E/T) ratio of 3:1, with the mAbs indicated at a final concentration of 10 μg/mL. (d) The HLA-DR8-negative B-LCL from the donor and an unrelated individual were transduced with mock or HLA-DRB1*08:03-encoding retroviral vector and tested with CTL-1H8 at an E/T ratio of 10:1.

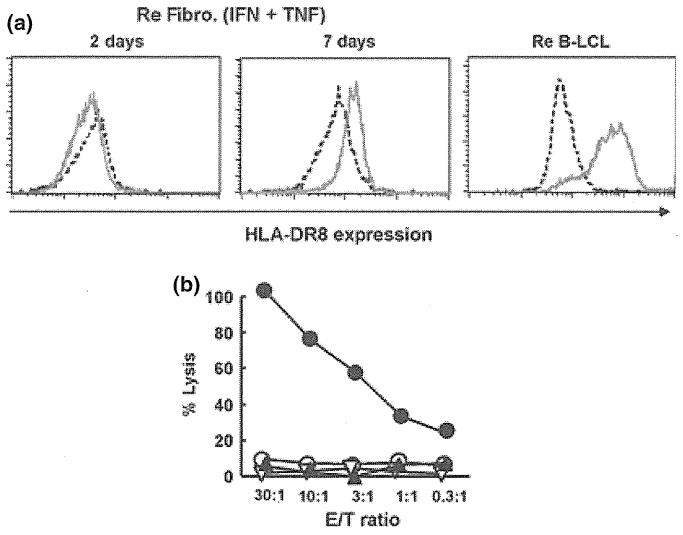

Fig. 2. Induction of human leukocyte antigen (HLA)-DR8 by cytokines and susceptibility of cytokine-treated dermal fibroblasts to CTL-1H8. (a) The recipient (Re) dermal fibroblasts (Fibro.) were incubated with 100 U/mL interferon (IFN)-γ and 10 ng/mL tumor necrosis factor (TNF)-α for 2 or 7 days and analyzed for HLA-DR8 expression with DR8-specific mAb. A recipient B-lymphoblastoid cell lines (B-LCL) was used as a positive control. (b) Recipient fibroblasts with or without 7 day cytokine treatment were tested for lysis by CTL-1H8 at indicated effector/target (E/T) ratios, in conjunction with recipient and donor (Do) B-LCL as positive and negative controls, respectively. (●), Re B-LCL; (○), Do B-LCL; (▽), Re Fibro.; (▲), Re Fibro. (IFN + TNF, 7 days.)

resulted in an approximate fourfold upregulation. However, the expression level was 1 log lower than that observed for recipient B-LCL (Fig. 2a, right panel). Despite HLA-DR8 upregulation, fibroblasts treated for 7 days were not lysed by CTL-1H8 at all (Fig. 2b), suggesting that the recognition of the HLA-DRB1*08:03 complex by CTL-1H8 may require HLA-bound antigenic peptides that are not produced in fibroblasts or that such weak upregulation may not be sufficient for recognition by CTL-1B8. The latter possibility may be less likely because primary ALL cells with similar HLA-DR8 expression were moderately lysed by CTL-1H8 (see below).

HLA-DR8 expression in primary leukemia cells and their susceptibility to CTL-1H8. Expression of DR8 on primary leukemia cells was first examined in conjunction with CD34, which has been shown to be a stem cell marker in humans.[13] Of 51 PBMC or BM specimens from leukemia patients, five had the HLA-DRB1*08:03 or DRB1*08:02 genotype, of which three samples contained a substantial fraction of CD34$^+$ cells, all of which were from patients with ALL (Ph-ALL: HLA-DRB1*08:02; B-ALL#1 and B-ALL-#2: HLA-DRB1*08:03), and had a significant fraction of double-positive cells (Fig. 3a). We next tested whether positively selected CD34$^+$ fractions from the three ALL samples (Fig. 3b) were susceptible to CTL-1H8. As shown in Figure 3(c), the CD34$^+$ fraction from all three ALL samples was lysed by CTL-1H8 and no natural killer activity against HLA-deficient K562 cells was observed. Although the Ph-ALL sample carried the HLA-DRB1*08:02 genotype, the cells were lysed by CTL-1H8, suggesting that the single amino acid difference in the HLA-DRB1 α1 domain between *08:03 and *08:02 did not affect recognition by CTL-1H8.

Inhibition of human Ph-positive ALL cell engraftment in NOG mice by CTL-1H8. In order to determine whether HLA-DR8 recognized by CTL-1H8 is indeed expressed on leukemic stem cells and thus may have been involved in a GVL effect, we performed the leukemic stem cell (LSC) engraftment assay, as reported previously,[14] using NOG mice.[4] Because we were unable to obtain CD34$^+$ fractions of primary leukemic cells from the present patient, we selected Ph-positive primary ALL (Ph-ALL) leukemic cells (positive for HLA-A*24:02 and DRB1*08:02) for this assay because they were found to be negative for the HLA-A*24:02-restricted minor histocompatibility antigen ACC-1C and were not lysed by the ACC-1C-specific clone CTL-1B9[8] (data not shown), which was used as an irrelevant control (see Materials and Methods). Flow cytometric analysis of the harvested cells was conducted to investigate the expression of human CD45 and CD34. The BM cells of three control mice receiving Ph-ALL CD34$^+$ cells that were cultured in medium alone (n = 1) or with control CTL-1B9 (n = 2) prior to inoculation were found to contain 96.5%, 32.9%, and 10.9% human CD45$^+$ CD34$^+$ cells (Fig. 4a–c), whereas the PBMC of the same three mice contained 65.2%, 5.7%, and 9.6% human CD45$^+$ CD34$^+$ cells (data not shown). In contrast, human cells were undetectable in both BM and PBMC of mice inoculated

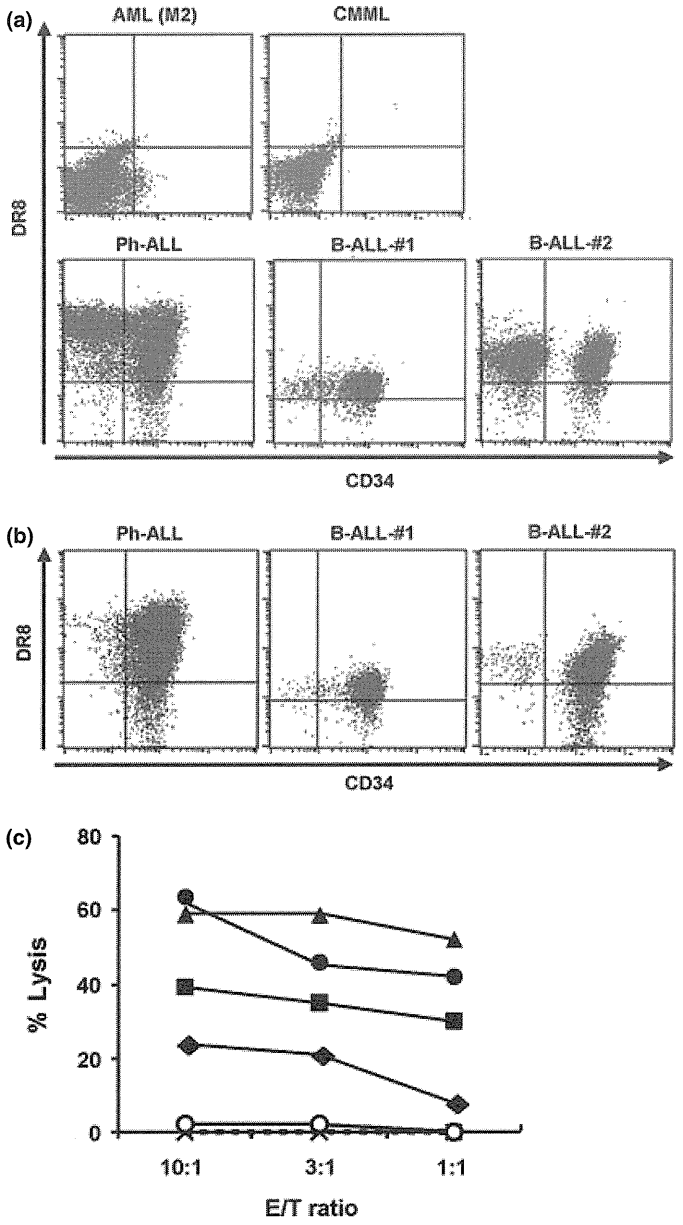

Fig. 3. Expression of human leukocyte antigen (HLA)-DR8 in primary leukemia cells and their susceptibility to CTL-1H8. (a) Expression of DR8 on five primary leukemia samples possessing the HLA-DRB1*08:02 or DRB1*08:03 genotype was examined in conjunction with CD34. (b) Purity and HLA-DR8 expression of leukemia cells after positive selection using anti-CD34-PE antibody followed by capture with anti-phycoerythrine (PE)-immunomagnetic beads. (c) Lysis of the $CD34^+$ fraction from all three acute lymphoblastic leukemia (ALL) samples by CTL-1H8, in conjunction with recipient (Re) and donor (Do) B-lymphoblastoid cell lines (B-LCL) as positive and negative controls, respectively. (●), Re B-LCL; (○), Do B-LCL; (▲), Philadelphia chromosome (Ph)-ALL; (■), B-ALL#1; (◇), B-ALL-#2; (×), K562. M2, French–American–British subtype M2; CMML, chronic myelomonocytic leukemia; E/T, effector/target. The HLA-DRB1 types of the three ALL samples were as follows: Ph-ALL, *08:02; B-ALL-#1, *08:03; and B-ALL-#2, 08:02.

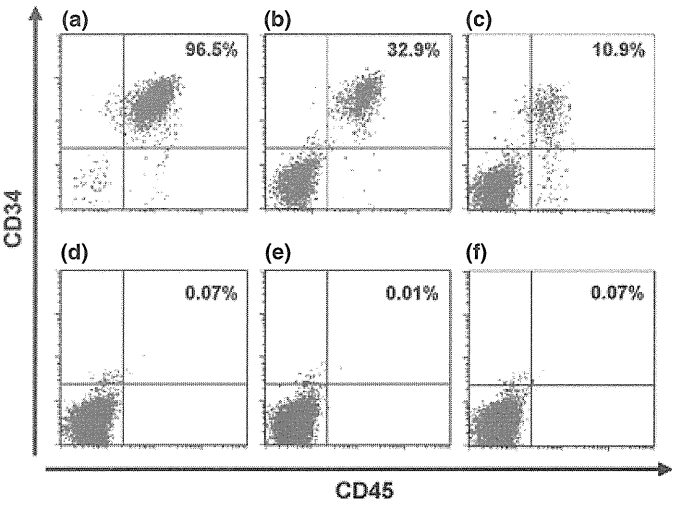

Fig. 4. Inhibition of human Philadelphia chromosome acute lymphoblastic leukemia (Ph-ALL) stem cell engraftment in non-obese diabetic/severe combined immunodeficient/γc-null (NOG) mice by CTL-1H8. The $CD34^+$ fraction (3.0×10^6) of a Ph-positive primary ALL sample was preincubated for 16 h either alone or in the presence of CTL-1H8 or a control CTL-1B9 (see Materials and Methods) and inoculated via the tail vein into 8–10-week-old NOG mice. Six to 7 weeks after inoculation, mice were killed and peripheral blood mononuclear cells and bone marrow (BM) cells were obtained. Flow cytometric profiles are shown for the expression of human CD45 and CD34 of BM cells from (a) control mice receiving Ph-ALL $CD34^+$ cells cultured in medium alone or (b,c) with control CTL-1B9 or (d–f) with CTL-1H8 prior to inoculation.

with Ph-ALL cells precultured with CTL-1H8 ($n = 3$; 0.07%, 0.01%, and 0.07% human $CD45^+$ $CD34^+$ cells in BM cells; Fig. 4d–f).

After HLA-DR mismatched HSCT, HLA-DR-specific $CD8^+$ T cells are detectable in recipient post-transplant PBMC. A split-well assay was used to estimate the relative frequencies of $CD8^+$ CTLp specific for HLA-DRB1*08:03 and those specific for all alloantigens expressed on the recipient's hematopoietic cells in the post-HSCT PBMC, as reported previously.[9] As shown in Figure 5 (left panel), the frequency of CTLp reactive with recipient B-LCL and HLA-DRB1*08:03-transfected donor B-LCL in peripheral blood $CD8^+$ cells obtained on Day 207 after HSCT, from which the CTL-1H8 was derived, was 1/1317 (95% confidence interval [CI] 1/906–1/1913) and 1/2689 (95% CI 1/1825–1/3961), respectively, indicating that nearly half the CTL responses to recipient alloantigens in this donor/recipient pair were directed at the mismatched HLA-DR8. On Day 355, the frequency of CTLp recognizing HLA-DRB1*08:03-transfected donor B-LCL was 1/22 580 (95% CI 1/14 241–1/35 801) and that for CTLp recognizing recipient B-LCL was 1/16 508 (95% CI 1/10 823–1/25 178), demonstrating that even at the later time point the $CD8^+$ CTL responses against HLA-DR8 continued to account for a significant fraction (73%) of the total donor CTL response in this donor/recipient pair (Fig. 5, right panel).

To explore whether our finding is a phenomenon limited to the present patient, we performed similar assays in another patient receiving cord blood HSCT mismatched by three loci (HLA-C, DR, and DQ). As indicated in Table 1, a small fraction (2.2–12.1% at three time points after HSCT) of the total donor $CD8^+$ CTL response in this donor/recipient pair was directed against the mismatched HLA-DRB1*12:01, whereas a slightly higher fraction (7.1–17.6%) was directed against the mismatched HLA-C*04:01. We were unable to examine the CTLp against the mismatched HLA-DQ molecule owing to an insufficient number of cells.

Discussion

To our knowledge, the present study is the first to demonstrate that $CD8^+$ CTL restricted by a mismatched HLA-DR molecule

doi: 10.1111/j.1349-7006.2011.01949.x

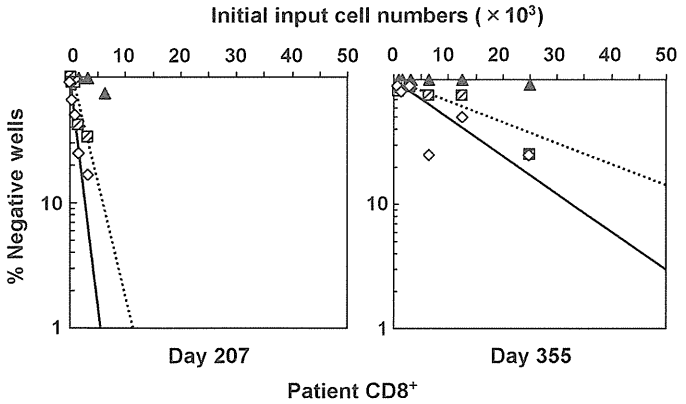

Fig. 5. Human leukocyte antigen (HLA)-DR8-specific $CD8^+$ T cells were detectable in recipient (Re) post-transplant peripheral blood mononuclear cells (PBMC) following HLA-DR-mismatched hematopoietic stem cell transplantation (HSCT). The proportion of $CD8^+$ CTL precursors specific for HLA-DRB1*08:03 among total CTL precursors (CTLp) against recipient alloantigens was quantitated using a standard limiting dilution assay with L-Calc software (StemCell Technologies, Vancouver, BC, Canada). The $CD8^+$ T cells from PBMC on Days 207 or 335 after HSCT were cultured at limiting dilution with irradiated CD40-B cells generated from pre-HSCT recipient PBMC in 96-well round-bottomed plates. After three rounds of stimulation, a split-well analysis was performed for HLA-DRB1*08:03-specific cytotoxicity against ^{51}Cr-radiolabeled recipient B-lymphoblastoid cell lines (B-LCL, -◇-) or donor B-LCL transduced with HLA-DRB1*08:03 cDNA (···▨···) or mock-transduced donor B-LCL (▲). Wells were considered positive if the total c.p.m. released by effector cells was >3 × SD above that in control wells.

Table 1. Frequency of $CD8^+$ cells against mismatched HLA-C and DR antigens in the population of CTL precursors

	Anti-Re	Anti-HLA-C*04:01 (%)	Anti-HLA-DRB1*12:01 (%)
Day 52	1/1882	1/26 651 (7.1)	1/26 101 (7.2)
Day 102	1/7577	1/84 290 (9.0)	1/346 830 (2.2)
1.3 years	1/16 807	1/95 577 (17.6)	1/139 331 (12.1)

The patient received cord blood transplantation for her T cell acute lymphocytic leukemia. Human leukocyte antigen (HLA) typing for the recipient (Re) and donor (Do) was as follows, with mismatched alleles underlined: Re: A*24:02/11:01, B*15:01/54:01, C*01:02/04:01, DRB1*04:06/12:01, DQB1*03:01/03:02, DPB1*02:01/03:01 Do: A*24:02/11:01, B*15:01/54*01, C*01:02/–, DRB1*04:06/05:05, DQB1*03:02/04:02, DPB1*02:01/*03:01. HLA, human leukocyte antigen.

are induced physiologically and can be cytotoxic against hematopoietic cells carrying the mismatched HLA-DR allele. The HLA-DRB1*08:03-restricted $CD8^+$ CTL-1H8 clone was isolated from a patient who received an HLA-DR-mismatched HSCT. At 207 days after HSCT, CTLp frequency analysis demonstrated that nearly half the $CD8^+$ T cell responses specific for any recipient-specific alloantigen were directed against the mismatched HLA-DRB1*08:03 molecule. Although we were unable to determine the magnitude of the $CD4^+$ T cell responses against the mismatched HLA-DRB1*08:03 molecule because of a paucity of PBMC, the $CD8^+$ CTLp frequency of 1/2689 on Day 207 is high enough to conclude that the isolation of CTL-1H8 was not an artifact. (The composition of the $CD8^+$ CTLp against mismatched HLA-DPB1*02:02 could not be determined in the present study, but it is possible that the remaining CTLp would be partly restricted by the HLA-DP or minor histocompatibility antigens restricted by shared HLA alleles. In this setting, the involvement of tumor antigens could not be assessed because the stimulators used in the present analysis were recipient CD40L-activated normal B cells and not leukemia cells.) This unexpected finding is supported by data from another HLA class I- and II-mismatched HSCT recipient. Because the number of patients receiving HLA-mismatched HSCT from various donors is increasing, it would be of interest to determine the kinetics of T cell reactions to individually mismatched HLA molecules depending on the type of hematopoietic stem cell donor.

It is generally believed that class II MHC-specific TCR transgenic mice predominantly give rise to $CD4^+$ T cells, whereas class I-specific TCR transgenic mice predominantly give rise to $CD8^+$ T cells. Furthermore, CD4 and CD8 are believed to activate T cells effectively when the intrinsic affinity of the TCR or antigen expression is low,[15] and these accessory molecules can work even if the interacting MHC is not directly bound to the self TCR.[16] In line with this, it has been shown that mature $CD8^+$ T cells can develop in class II MHC-specific TCR transgenic mice when CD4 is absent[17] and that polyclonal $CD4^+$ T cells transduced with the TCR molecules cloned from a $CD8^+$ WT1-specific T cell clone can lyse and/or react with their target cells.[18] In addition, the allorecognition of MHC class II molecules by $CD8^+$ T cells prepared from class II-deficient mice,[19] by those stimulated with antigen-specific B cells,[20] and by heteroclitic $CD8^+$ T cells that also recognize a class I[21] have been described. These findings imply the flexibility of coreceptor choice under unusual conditions. Thus, HLA-mismatched HSCT could be one such unusual situation where T cells may fail to follow the lineage instruction in the thymus because of highly inflammatory and immunogenic conditions after HLA-mismatched allo-HSCT.

Leukemic stem cells have a particularly strong capacity for proliferation, differentiation, and self-renewal[22] and likely play an important role in disease relapse after HSCT. Our mouse model clearly demonstrated that at least HLA-DRB1*08:03 is expressed on such stem cells and may serve as a GVL target for CTL-1H8 *in vivo*. Unfortunately, however, we could not confirm the GVL potential of CTL-1H8 against recipient leukemia cells because of a limited number of leukemia cells cryopreserved at the time of diagnosis. Because it has been shown that AML (M6) cells do not always express either HLA-DR and CD34,[23] it would need to be determined whether a small fraction of patient stem cells coexpress both HLA-DR and CD34. Nevertheless, it is of note that targeting an HLA-DR molecule alone using a specific CTL clone was sufficient to inhibit Ph-ALL LSC engraftment, suggesting that most LSC were present in the HLA-DR strongly positive, and not weakly positive or negative, population (Ph-ALL in Fig. 3b).

Finally, GVHD is still the major cause of mortality and morbidity following allo-HSCT. Therefore, selective induction of GVL is crucial. Under less inflammatory conditions, MHC class II molecules are mainly expressed only on hematopoietic cells, including leukemia cells. Thus, targeting HLA-DR molecules could be an ideal approach for this purpose. The patient in the present study has been free of disease recurrence for more than 2 years, but developed grade II aGVHD and extensive chronic GVHD. At least in the Japanese population, it has been shown that disparity in HLA-DR is much less hazardous than that in HLA-A and -B in terms of the development of severe aGVHD and mortality.[2] It remains to be determined in future studies whether targeting a mismatched HLA-DR molecule, especially late after HSCT when inflammatory conditions have subsided, would induce detrimental GVHD. In addition, the potential targeting of an HLA-DP molecule whose disparity is almost permissive following HSCT[2] should be examined.

Acknowledgments

The authors thank Dr William Ho (Exploratory Clinical Development, Genentech, South San Francisco, USA) for critically reading the manuscript. The authors also thank Miwako Nishizawa and Hiromi Tamaki for their expert technical assistance and Drs Hiroo Saji and Etsuko Maruya (HLA Laboratory, Kyoto, Japan) for valuable suggestions regarding HLA typing. This study was supported, in part, by the Third Term Comprehensive Control Research for Cancer (no. 30) and Research on Allergic Disease and Immunology from the Ministry of Health, Labour, and Welfare, Japan, as well as Grants-in-Aid for Scientific Research (C) (no. 21591256) from the Ministry of Education, Culture, Science, Sports, and Technology, Japan.

Disclosure Statement

The authors declare no competing financial interests.

References

1 Kernan NA, Bartsch G, Ash RC *et al.* Analysis of 462 transplantations from unrelated donors facilitated by the National Marrow Donor Program. *N Engl J Med* 1993; **328**: 593–602.
2 Kawase T, Morishima Y, Matsuo K *et al.* High-risk HLA allele mismatch combinations responsible for severe acute graft-versus-host disease and implication for its molecular mechanism. *Blood* 2007; **110**: 2235–41.
3 Garcia KC, Degano M, Speir JA, Wilson IA. Emerging principles for T cell receptor recognition of antigen in cellular immunity. *Rev Immunogenet* 1999; **1**: 75–90.
4 Ito M, Hiramatsu H, Kobayashi K *et al.* NOD/SCID/gamma(c) (null) mouse: an excellent recipient mouse model for engraftment of human cells. *Blood* 2002; **100**: 3175–82.
5 Kondo E, Topp MS, Kiem HP *et al.* Efficient generation of antigen-specific cytotoxic T cells using retrovirally transduced CD40-activated B cells. *J Immunol* 2002; **169**: 2164–71.
6 Watanabe K, Suzuki S, Kamei M *et al.* CD137-guided isolation and expansion of antigen-specific CD8 cells for potential use in adoptive immunotherapy. *Int J Hematol* 2008; **88**: 311–20.
7 Riddell SR, Greenberg PD. The use of anti-CD3 and anti-CD28 monoclonal antibodies to clone and expand human antigen-specific T cells. *J Immunol Methods* 1990; **128**: 189–201.
8 Kawase T, Nannya Y, Torikai H *et al.* Identification of human minor histocompatibility antigens based on genetic association with highly parallel genotyping of pooled DNA. *Blood* 2008; **111**: 3286–94.
9 Torikai H, Akatsuka Y, Miyazaki M *et al.* A novel HLA-A*3303-restricted minor histocompatibility antigen encoded by an unconventional open reading frame of human TMSB4Y gene. *J Immunol* 2004; **173**: 7046–54.
10 Akatsuka Y, Morishima Y, Kuzushima K, Kodera Y, Takahashi T. Minor histocompatibility antigens as targets for immunotherapy using allogeneic immune reactions. *Cancer Sci* 2007; **98**: 1139–46.
11 Matsushita M, Yamazaki R, Ikeda H *et al.* Possible involvement of allogeneic antigens recognised by donor-derived CD4 cytotoxic T cells in selective GVL effects after stem cell transplantation of patients with haematological malignancy. *Br J Haematol* 2006; **132**: 56–65.
12 Griffioen M, van der Meijden ED, Slager EH *et al.* Identification of phosphatidylinositol 4-kinase type II beta as HLA class II-restricted target in graft versus leukemia reactivity. *Proc Natl Acad Sci U S A* 2008; **105**: 3837–42.
13 Krause DS, Fackler MJ, Civin CI, May WS. CD34: structure, biology, and clinical utility. *Blood* 1996; **87**: 1–13.
14 Kawase T, Akatsuka Y, Torikai H *et al.* Alternative splicing due to an intronic SNP in HMSD generates a novel minor histocompatibility antigen. *Blood* 2007; **110**: 1055–63.
15 de Vries JE, Yssel H, Spits H. Interplay between the TCR/CD3 complex and CD4 or CD8 in the activation of cytotoxic T lymphocytes. *Immunol Rev* 1989; **109**: 119–41.
16 Lustgarten J, Waks T, Eshhar Z. CD4 and CD8 accessory molecules function through interactions with major histocompatibility complex molecules which are not directly associated with the T cell receptor-antigen complex. *Eur J Immunol* 1991; **21**: 2507–15.
17 Matechak EO, Killeen N, Hedrick SM, Fowlkes BJ. MHC class II-specific T cells can develop in the CD8 lineage when CD4 is absent. *Immunity* 1996; **4**: 337–47.
18 Tsuji T, Yasukawa M, Matsuzaki J *et al.* Generation of tumor-specific, HLA class I-restricted human Th1 and Tc1 cells by cell engineering with tumor peptide-specific T cell receptor genes. *Blood* 2005; **106**: 470–6.
19 Shimizu T, Takeda S. CD8 T cells from major histocompatibility complex class II-deficient mice respond vigorously to class II molecules in a primary mixed lymphocyte reaction. *Eur J Immunol* 1997; **27**: 500–8.
20 Shinohara N, Watanabe M, Sachs DH, Hozumi N. Killing of antigen-reactive B cells by class II-restricted, soluble antigen-specific $CD8^+$ cytolytic T lymphocytes. *Nature* 1988; **336**: 481–4.
21 Schilham MW, Lang R, Benner R, Zinkernagel RM, Hengartner H. Characterization of an Lyt-2+ alloreactive cytotoxic T cell clone specific for H-2Db that cross-reacts with I-Ek. *J Immunol* 1986; **137**: 2748–54.
22 Bonnet D, Warren EH, Greenberg PD, Dick JE, Riddell SR. CD8(+) minor histocompatibility antigen-specific cytotoxic T lymphocyte clones eliminate human acute myeloid leukemia stem cells. *Proc Natl Acad Sci U S A* 1999; **96**: 8639–44.
23 Khalidi HS, Medeiros LJ, Chang KL, Brynes RK, Slovak ML, Arber DA. The immunophenotype of adult acute myeloid leukemia: high frequency of lymphoid antigen expression and comparison of immunophenotype, French–American–British classification, and karyotypic abnormalities. *Am J Clin Pathol* 1998; **109**: 211–20.

doi: 10.1111/j.1349-7006.2011.01949.x

Biochemical and Biophysical Research Communications 405 (2011) 405–410

Contents lists available at ScienceDirect

Biochemical and Biophysical Research Communications

journal homepage: www.elsevier.com/locate/ybbrc

The reconstituted 'humanized liver' in TK-NOG mice is mature and functional

Masami Hasegawa [a,d,g], Kenji Kawai [b], Tetsuya Mitsui [f], Kenji Taniguchi [a,g], Makoto Monnai [a,h], Masatoshi Wakui [b,d,e], Mamoru Ito [c], Makoto Suematsu [d], Gary Peltz [i], Masato Nakamura [b,j], Hiroshi Suemizu [a,*]

[a] Biomedical Research Department, Central Institute for Experimental Animals, 1430 Nogawa, Miyamae, Kawasaki, Kanagawa 216-0001, Japan
[b] Pathology Research Department, Central Institute for Experimental Animals, 1430 Nogawa, Miyamae, Kawasaki, Kanagawa 216-0001, Japan
[c] Laboratory Animal Research Department, Central Institute for Experimental Animals, 1430 Nogawa, Miyamae, Kawasaki, Kanagawa 216-0001, Japan
[d] Department of Biochemistry and JST ERATO Suematsu Gas Biology Project, Keio University School of Medicine, 35 Shinanomachi, Shinjuku, Tokyo 160-8582, Japan
[e] Department of Laboratory Medicine, Keio University School of Medicine, 35 Shinanomachi, Shinjuku, Tokyo 160-8582, Japan
[f] Pre-Clinical Research Department, Chugai Pharmaceutical Co., Ltd., 1-135 Komakado, Gotemba, Shizuoka 412-8513, Japan
[g] Pharmaceutical Research Department II, Chugai Pharmaceutical Co., Ltd., 200 Kajiwara, Kamakura, Kanagawa 247-8530, Japan
[h] Chugai Research Institute for Medical Science, Inc., 200 Kajiwara, Kamakura, Kanagawa 247-8530, Japan
[i] Department of Anesthesia, Stanford University, Stanford, CA 94305-5796, USA
[j] Department of Pathology, Tokai University School of Medicine, 143 Shimokasuya, Isehara, Kanagawa 259-1193, Japan

ARTICLE INFO

Article history:
Received 20 December 2010
Available online 14 January 2011

Keywords:
Humanized mouse
Liver reconstitution
Herpes simplex virus type 1 thymidine kinase (HSVtk)
Drug metabolism

ABSTRACT

To overcome the limitations of existing models, we developed a novel experimental *in vivo* platform for replacing mouse liver with functioning human liver tissue. To do this, a herpes simplex virus type 1 thymidine kinase (HSVtk) transgene was expressed within the liver of highly immunodeficient NOG mice (TK-NOG). Mouse liver cells expressing this transgene were ablated after a brief exposure to a non-toxic dose of ganciclovir (GCV), and transplanted human liver cells are stably maintained within the liver (humanized TK-NOG) without exogenous drug. The reconstituted liver was shown to be a mature and functioning "human organ" that had zonal position-specific enzyme expression and a global gene expression pattern representative of mature human liver; and could generate a human-specific profile of drug metabolism. The 'humanized liver' could be stably maintained in these mice with a high level of synthetic function for a prolonged period (8 months). This novel *in vivo* system provides an optimized platform for studying human liver physiology, including drug metabolism, toxicology, or liver regeneration.

1. Introduction

We [1] and other groups [2,3] have produced immunocompromised mice with human liver tissue as model system for analysis of drug metabolism and liver regeneration. In several models, human liver cells are transplanted into immunodeficient mice that express a urokinase-type plasminogen activator (uPA) transgene in their liver. Remarkably, human-specific hepatitis viruses can infect these mice [2–4]; their reconstituted livers express enzymes found in human liver cells [5]; and they can generate human-specific metabolites of test substrates, including steroids [6–10]. Although uPA expression facilitates the growth of transplanted human liver cells; it causes continuing and progressive damage to liver parenchymal cells, possibly via activation of plasminogen, which regulates the activity of matrix metalloproteinases that are critical for liver cell growth. Thus, these uPA-dependent models have very significant disadvantages that limit their utility for many applications, including a very poor breeding efficiency, renal disease, and a very narrow time window for transplantation before the mice succumb to their bleeding diathesis. A fumarylacetoacetate hydrolase (*Fah*) knockout mouse [11] has also been utilized for this purpose. In some instances, this model also requires (virus-mediated) uPA expression in liver to facilitate human hepatocyte transplantation, and thus has the same limitations. *Fah* mice also develop liver carcinomas as a consequence of their type I tyrosinemia, and continued or intermittent drug treatment after humanization is required to suppress the development of liver cancer, which enables their long term survival [4]. As a consequence, analyses of drug metabolism or liver regeneration in these models are confounded by the ongoing liver pathology or by the requirement for continued drug treatment. Therefore, we utilized a substantially different approach to overcome these limitations. The targeted expression of the herpes simplex virus type 1 thymidine kinase (HSVtk) in the liver of

Abbreviations: CK8/18, human Cytokeratin (8/18); DEB, debrisoquine; Fah, fumarylacetoacetate hydrolase; GCV, ganciclovir; H&E, hematoxylin and eosin; hAlb, human albumin; HSVtk, herpes simplex virus type 1 thymidine kinase; MIAME, minimum information about a microarray experiment; nHeps, normal human liver cells; RI, replacement index; RT-PCR, reverse transcription-PCR; uPA, urokinase-type plasminogen activator.

* Corresponding author. Fax: +81 44 754 4465/4454.
E-mail address: suemizu@ciea.or.jp (H. Suemizu).

0006-291X/$ - see front matter © 2011 Elsevier Inc. All rights reserved.
doi:10.1016/j.bbrc.2011.01.042

severely immunodeficient NOG mice enabled mouse liver to be stably replaced with mature and functional human liver tissue in the absence of ongoing drug treatment.

2. Materials and methods

2.1. Transgenic mice, human liver cell transplantation and drug biotransformation analysis

The herpes simplex virus type 1 thymidine kinase (*UL23* or HSVtk) gene expression unit was constructed as in Fig. S1A. A vector-free 4.4-kb HSVtk expression fragment was microinjected into fertilized NOD/Shi strain mouse eggs using standard methods. For further information about the creation and breeding of the TK-NOG strain, human liver cell transplantation, and the drug biotransformation studies, see supplementary materials and methods. This study was performed in accordance with institutional guidelines and was approved by the Animal Experimentation Committee of the Central Institute for Experimental Animals.

2.2. Histology and immunohistochemistry

Formalin-fixed and paraffin embedded (5 μm) sections were used for immunohistochemical staining with Cytokeratin (8/18) (h-CK8/18), HLA class I-A, B, C, asialoglycoprotein receptor 1 (ASGR1), albumin, glutamine synthetase (GS) antibodies. To estimate the replacement index (RI), which is the percentage of donor human liver cells in recipient livers, the ratio of the area occupied by h-CK8/18-positive cells to the entire area examined in immunohistochemical sections of three to five lobes was measured.

2.3. Immunoblotting

Human albumin, complement C3 protein, transferrin, and ceruloplasmin secretion was analyzed by Immunoblotting with specific primary antibodies and horseradish peroxidase-labeled secondary antibodies. The general information about the antibodies used for detection of the human protein are provided in the supplementary materials and methods.

2.4. Oligonucleotide array hybridization

Global gene expression was analyzed using the HG-U133A Plus 2 GeneChip array (Affymetrix Inc., Santa Clara, CA). Signal intensity for each transcript (background subtracted and adjusted for noise) and detection call (present, absent, or marginal) were determined using Affymetrix Expression Console Software (Affymetrix Inc.). The signal was normalized by house keeping gene, the human 18S rRNA gene (10098_M_at probe). The MIAME compliant microarray data was deposited in the Center for Information Biology gene EXpression database (CIBEX) at DDBJ (Japan) (CIBEX Accession: CBX102).

2.5. Statistical analyses

Statistical analyses were performed with the Prism 5 software (GraphPad Software, CA, USA) and SAS preclinical package software ver. 5.0 (SAS Institute, Tokyo, Japan).

3. Results

3.1. A reconstituted 'humanized liver' in TK-NOG mice can be stably maintained

Targeted HSVtk expression has previously been used to ablate specific cell types in transgenic mice [12–14]. Therefore, we used an albumin promoter to drive the liver-specific expression of a HSVtk transgene in severely immunodeficient NOG mice [15] to produce TK-NOG mice. Administration of GCV, a drug that is not toxic to human or mouse tissues, induces tissue-specific ablation of transgenic liver parenchymal cells. Since HSVtk catalyzes GCV phosphorylation, which is the rate-limiting step that cannot be performed in mammalian cells lacking this transgene, liver cells expressing the transgene are selectively destroyed. The HSVtk transgene construct, mouse breeding, protocol variables, and the properties of TK-NOG mice are described in the supplementary information and in Fig. S1. We developed an initial protocol that enabled transplanted human liver cells to replace mouse liver. A dose of GCV (0.5–5 mg/kg I.P) that is not toxic to human or mouse tissues was administered on days seven and five prior to transplantation, and 10^6 human liver cells were transplanted via intra-splenic injection. Despite using a non-optimized protocol in the initial pilot studies, a substantial amount of human albumin (hAlb) was detected in the plasma obtained from all 123 TK-NOG recipients after human liver cell transplantation, and the hAlb levels increased steadily to a maximal plasma concentration of 5.9 mg/mL (average 1.5 mg/mL; Table 1; Fig. S2A). The extent of human liver replacement was highly correlated with the measured hAlb levels ($r^2 = 0.9471$; Fig. S2B), and the engrafted human liver cells were incorporated into the existing liver in recipient ('humanized' TK-NOG) mice (Fig. 1A). After optimization of the variables (age of mice at time of transplantation, dose/timing of GCV administration) as described in the supplementary information and Fig. S3, the hAlb concentration (average 3.3 mg/mL) and level of human engraftment (average 43%) in TK-NOG mice was substantially increased (Table 1). It has recently been reported that transplantation of an increased number of human cells increases the level of human liver chimerism in $Fah^{-/-}$ model [4]. However, the average level of human reconstitution (43%) in TK-NOG liver is already at or above that obtained when this modification was used in the $Fah^{-/-}$ mouse. However, it is possible that increasing the number of transplanted human cells could further increase liver chimerism in TK-NOG mice.

Of importance, the 'humanized' TK-NOG livers maintained their synthetic function for a prolonged period. Humanized TK-NOG mice maintained a very high plasma hAlb level over a 8-month period of observation, and did not experience any loss of body weight (Fig. 1B). The functioning human liver was maintained despite the fact these mice did not receive any medication other than the GCV, which was administered prior to transplantation. This prolonged period of human liver survival has not been achieved

Table 1
Engraftment of human liver cells and repopulation rates in chimeric mice using a pilot or optimized transplantation protocol.

Pilot		Optimized		
Mice (n)	hAlb (mg/mL)	Mice (n)	hAlb (mg/mL)	Chimerism (%)
39	0.2	5	0.8	13.4
26	0.7	14	1.6	22.5
29	1.5	8	3.3	41.9
18	3.2	10	4.5	55.7
8	4.7	1	6.9	83.1
3	5.7	5	7.8	93.4
Total, 123	Average, 1.5	Total, 43	Average, 3.3***	Average, 42.5

The amount of human albumin (hAlb) in plasma and extent of human liver replacement was measured after TK-NOG mice were transplanted with human liver cells using non-optimized pilot or optimized protocols. The extent of human liver chimerism was estimated as a function of the hAlb concentration, which was shown to correlate with the extent of human liver replacement. Protocol optimization (age at time of transplantation and GCV regimen) significantly increased the extent of humanization relative to that obtained in the pilot studies.
*** Mann–Whitney test, difference of $P < 0.0001$.